European Journal of Medicinal Chemistry 304 (2026) 118506

Contents lists available at ScienceDirect

European Journal of Medicinal Chemistry

journal homepage: www.elsevier.com/locate/ejmech

Research paper

Discovery of antileishmanial hits in the 3-nitroimidazo[1,2-*a*]pyridine series via newly optimized tetrakis(dimethylamino)ethylene (TDAE) methodology at position 2

Inès Jacquet [a], Romain Paoli-Lombardo [a,b], Caroline Castera-Ducros [a,b], Hugo Pomares [a], Sandra Bourgeade-Delmas [c], Patrice Vanelle [a,b,*], Nicolas Primas [a,b,**]

[a] Aix Marseille Univ, CNRS, ICR UMR 7273, Team Pharmaco-Chimie Radicalaire, Faculté de Pharmacie, 27 Boulevard Jean Moulin, CS30064, CEDEX 05, Marseille, 13385, France
[b] Service Central de la Qualité et de l'Information Pharmaceutiques, Hôpital de la Conception, AP-HM, Marseille, 13005, France
[c] UMR 152 Pharma Dev, Université de Toulouse, IRD, UPS, Toulouse, 31062, France

ARTICLE INFO

Keywords:
3-Nitroimidazo[1,2-*a*]pyridine
TDAE
N-Tosylbenzylimine
Leishmania
Nitroaromatic compounds
Nucleophilic aromatic substitution
Palladium-catalyzed cross-coupling

ABSTRACT

To explore the antileishmanial structure-activity relationships at position 2 of the 3-nitroimida-zo[1,2-*a*]pyridine scaffold, we developed a new synthetic method using Tetrakis(dimethylamino)ethylene (TDAE) and *N*-tosyl-benzylimines. This original synthetic route was optimized to provide simple and reproducible access to diverse analogues functionalized at position 2. A library of 25 new derivatives was generated via efficient diversification at position 8 using nucleophilic aromatic substitution (S_NAr) and Suzuki–Miyaura cross-coupling reactions. The 8-brominated analogues emerged as the most promising series, with six compounds exhibiting submicromolar activity against *Leishmania infantum* axenic amastigotes. Further substitution at position 8 with 4-pyridinyl or *para*-chlorothiophenol groups significantly decreased potency. The most active compound was also active on intramacrophagic amastigotes (half maximal inhibitory concentration (IC_{50}) = 0.35 μM) without displaying any cytotoxicity on THP1 cell line (50 % cytotoxic concentration (CC_{50}) > 100 μM). The reduction of its nitro group afforded an amino analogue, which retained antileishmanial activity (IC_{50} = 2.77 μM), indicating potential alternative mechanisms of action beyond nitro bioactivation. Despite its low solubility (<1 μM), this scaffold represents a novel and versatile entry point for antileishmanial drug discovery.

1. Introduction

According to the World Health Organization (WHO), Neglected Tropical Diseases (NTDs) are defined as a heterogeneous group of 21 conditions caused by a wide variety of pathogens, including bacteria, viruses, parasites, fungi, and toxins [1]. It is estimated that approximately 1.5 billion people are affected by NTDs worldwide. These conditions are predominantly observed in populations experiencing socio-economic vulnerability within tropical and subtropical regions.

Among the NTDs, leishmaniases are a group of zoonotic infectious diseases caused by a flagellated protozoan of the order *Kinetoplastida* and the genus *Leishmania* [2]. These parasites are vectorized by a hematophagous insect, specifically the female phlebotomine sandfly. In humans, they are found inside the macrophages in their amastigote form.

The clinical manifestations of leishmaniases exhibit notable variability, depending on various factors, including the specific parasitic species, the vector species, and the immune response of the human host. They typically present in three primary clinical forms: cutaneous, mucocutaneous, and visceral (or kala-azar) [3]. Cutaneous and

* Corresponding author. Aix Marseille Univ, CNRS, ICR UMR 7273, Team Pharmaco-Chimie Radicalaire, Faculté de Pharmacie, 27 Boulevard Jean Moulin, CS30064, CEDEX 05, Marseille, 13385, France.
** Corresponding author. Aix Marseille Univ, CNRS, ICR UMR 7273, Team Pharmaco-Chimie Radicalaire, Faculté de Pharmacie, 27 Boulevard Jean Moulin, CS30064, CEDEX 05, Marseille, 13385, France.
E-mail addresses: ines.jacquet@etu.univ-amu.fr (I. Jacquet), romain.paoli-lombardo@univ-amu.fr (R. Paoli-Lombardo), caroline.ducros@univ-amu.fr (C. Castera-Ducros), hugpomares@gmail.com (H. Pomares), sandra.bourgeade-delmas@ird.fr (S. Bourgeade-Delmas), patrice.vanelle@univ-amu.fr (P. Vanelle), nicolas.primas@univ-amu.fr (N. Primas).

https://doi.org/10.1016/j.ejmech.2025.118506
Received 7 October 2025; Received in revised form 4 December 2025; Accepted 17 December 2025
Available online 19 December 2025

mucocutaneous leishmaniasis are the most prevalent forms of the disease, with nearly one million new cases each year. Clinically, these conditions manifest as lesions on the skin and/or mucous membranes, resulting in persistent scarring and social stigmatization, which may lead to social exclusion of affected patients. Visceral leishmaniasis is an opportunistic form of the disease, primarily affecting children and immunocompromised individuals. It is characterized by symptoms such as irregular fever, weight loss, anemia, and hepatosplenomegaly. If left untreated, it leads to fatal bacterial superinfection or disseminated intravascular coagulation (DIC), which causes approximately 30,000 deaths per year. Despite undergoing treatment and achieving apparent clinical remission, post-kala-azar dermal leishmaniasis (PKDL) remains a potential complication, characterized by the development of debilitating skin lesions with social and psychological implications.

The arsenal of therapeutics for treating leishmaniasis is limited to a few molecules with numerous limitations (Scheme 1) [4]. Pentavalent antimony compounds, such as meglumine antimoniate and sodium stibogluconate, have serious side effects, including potentially fatal cardiotoxicity. Paromomycin has a high rate of resistance, and it requires repeated painful intramuscular injections. Liposomal amphotericin B is better tolerated but requires strict adherence to the cold chain and costs several hundred to thousands of US dollars for a full course of treatment. Miltefosine is the only oral treatment, but it is teratogenic and causes severe digestive side effects that limit treatment adherence.

Regarding anti-leishmaniasis drug research, DNDi lists only five new drug candidates in clinical trials (Scheme 2), four of which target the deadly visceral form of the disease [5]. One drug candidate has had its development halted due to side effects, reducing the number of drug candidates in clinical trials to three. This highlights the need for new oral treatments devoid of side effects.

Among the chemical classes that show potential for treating parasitic infections, nitroaromatics play a significant role. Their activity is associated with the bioactivation of their nitro group by parasitic nitroreductases [6,7]. These enzymes, which are essential to *Leishmania* but are absent in humans, catalyze successive reductions of the nitro group, generating toxic metabolites such as nitrenium ions and reactive oxygen species, which can damage the parasite's DNA and ultimately lead to its death.

The development of this class has long been hindered by its positivity in the Ames test, a genotoxicity assay using prokaryotes expressing nitroreductases. However, the implementation of novel mutagenicity tests in eukaryotic cells, such as the comet assay or the micronucleus test, led to a reevaluation of the safety profile of nitroaromatics, thereby stimulating renewed interest in their development [8]. Specifically, fexinidazole, a 5-nitroimidazole derivative, has recently been approved for the treatment of sleeping sickness, an NTD caused by *Trypanosoma brucei*, a parasite of the kinetoplastid family (Scheme 3) [9,10]. Another compound, DNDI-0690, a 2-nitroimidazole derivative, was evaluated in clinical trials against leishmaniasis until 2022 (Scheme 3) [11]. Despite the demonstration of encouraging activity, its development was suspended due to the identification of biological anomalies, however, the precise nature of these anomalies has not been disclosed.

The research conducted in our laboratory focuses on the antileishmanial potential of the 3-nitroimidazo[1,2-*a*]pyridine scaffold, which belongs to the family of nitroaromatics. In 2013, a screening revealed promising antileishmanial activity for several compounds in this chemical series [12].

This led to the development of more active analogues in subsequent years. Notably, in 2019 and 2020, two hit compounds were identified: hit **(A)**, bearing a chlorine atom at position 6, bromine atom at position 8 and a methylphenylsulfonyl group at position 2 [13]; and hit **(B)**, bearing a chlorine atom at position 6, a methylphenylsulfonyl group at position 2, and a 4-chlorophenylthioether group at position 8 (Scheme 4) [14]. Both compounds exhibited good *in vitro* antileishmanial activity and limited cytotoxicity.

Subsequent efforts focused on enhancing the physicochemical and *in vitro* pharmacokinetic properties, to the identification of hit **(C)** in 2022 [15]. This compound, which is substituted at position 2 by a methylsulfonyl-*gem*-trifluoropropyl chain and at position 8 by a pyridin-4-yl group, showed improved pharmacokinetic properties but lower antileishmanial activity (Scheme 4).

Further experiments demonstrated that hit **(B)** undergoes rapid *in vivo* bioreduction of the nitro group at position 3 to the corresponding amine, leading to a loss of activity. This reduction can be estimated using cyclic voltammetry, by measuring the reduction potential (E_0) of the nitro group. Indeed, clinically used nitroaromatic drugs exhibit an E_0 values close to −0.80 V (such as fexinidazole, with an E_0 of −0.83 V), while hits **(A)**, **(B),** and **(C)** display E_0 values in the range of −0.65 to −0.61 V.

Theoretically, tuning the electronic properties at position 2 could allow modulation of the E_0 and potentially improve metabolic stability. However, the methylsulfone substituents currently used strongly limit this modulation. The primary objective of this study was to explore an alternative synthetic strategy for further functionalizing the position 2 of the 3-nitroimidazo[1,2-*a*]pyridine ring.

We used tetrakis(dimethylamino)ethylene (TDAE), an organic reducing agent with the specific property of activating the carbon-halogen bond to generate a carbanion. Since 2002, our team has developed several reactions between nitroheterocyclic substrates and various electrophiles, such as carbonyls and *N*-tosylbenzylimines, using

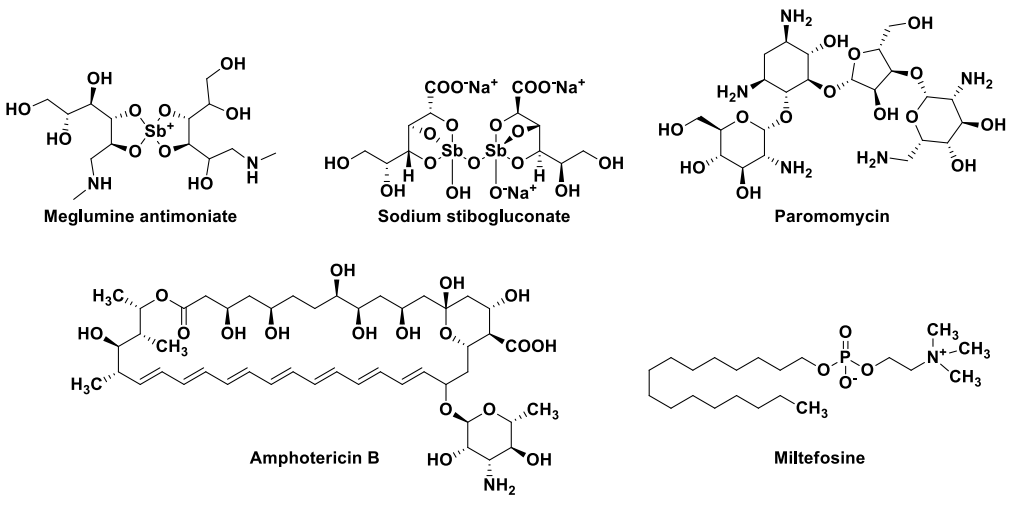

Scheme 1. Structures of antileishmanial treatments: Meglumine antimoniate, Sodium stibogluconate, Paromomycin, Amphotericin B and Miltefosine.

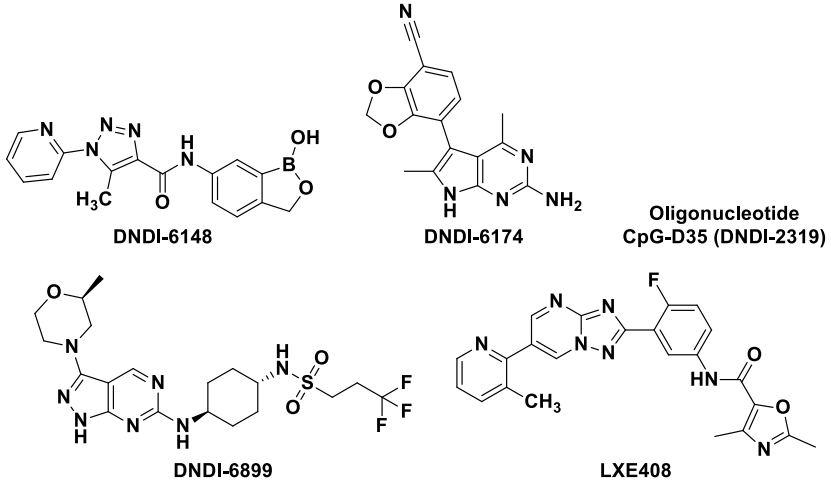

Scheme 2. Structures of drug candidates in antileishmanial clinical trials.

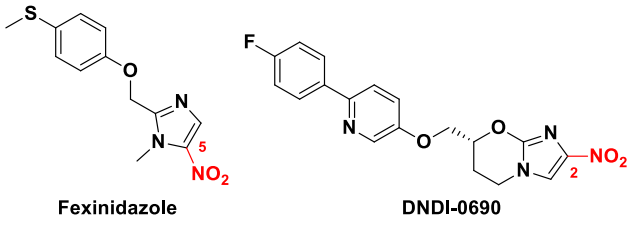

Scheme 3. Structures of nitro derivatives Fexinidazole and DNDI-0690.

the TDAE methodology [16]. This strategy was successfully used on position 2 of the 3-nitroimidazo[1,2-*a*]pyridine ring with α-ketomalonate in 2008 [17].

We optimized a new synthetic pathway using the TDAE methodology and other reactants, namely *N*-tosylbenzylimines, and synthesized a series of novel derivatives **(4a–k)**. Furthermore, the newly formed derivatives underwent late-stage modifications at position 8, approaching the structures of previously described hits **(B)** and **(C)**. A total of 25 compounds were synthesized and evaluated for *in vitro* antileishmanial activity and cytotoxicity. Subsequently, the E_0 of several compounds was measured, and the *in vitro* physicochemical and pharmacokinetic properties of the most potent antileishmanial compound were assessed.

2. Results

2.1. Synthesis

The 8-Bromo-6-chloro-2-chloromethyl-3-nitroimidazo[1,2-*a*]pyridine **(2)** was obtained via a two-step synthesis previously developed in our laboratory (Scheme 5). Commercially available 2-amino-3-bromo-5-chloropyridine was engaged in a cyclocondensation reaction with 1,3-dichloroacetone in refluxing ethanol to give intermediate **(1)**, followed by a nitration reaction at position 3 to obtain intermediate **(2)**.

Although the TDAE-mediated functionalization of position 2 of the 3-nitroimidazo[1,2-*a*]pyridine scaffold was previously demonstrated using α-ketomalonate, this transformation was performed on an unsubstituted ring [17]. In the present study, substitution at position 8 was considered essential to align with the previously identified bioactive scaffold.

To assess whether such a substitution would interfere with the reactivity of the scaffold, a model reaction was first carried out using diethyl oxomalonate under the previously reported conditions, starting from intermediate **(2)**, which bears a bromine atom at position 8. The reaction proceeded smoothly, yielding compound **(3)** in 45 % yield (Scheme 6).

This outcome demonstrates that the presence of a substituent at position 8 does not significantly hinder the formation of the carbanion

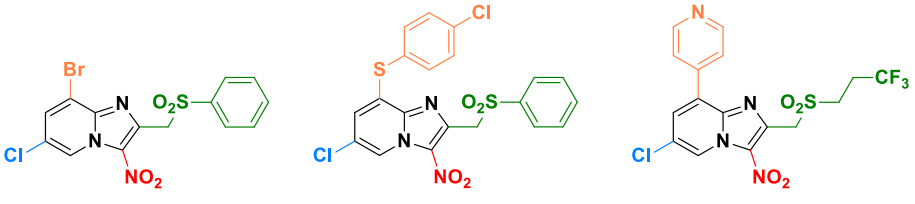

	Hit **(A)**	Hit **(B)**	Hit **(C)**
CC_{50} THP1 (μM)	> 100	> 62.5	> 100
IC_{50} *L. infantum* axenic amastigotes (μM)	16.4	1.7	14.0
IC_{50} *L. infantum* intramacrophagic amastigotes (μM)	2.1	3.2	3.7
E_0 (V)	-0.65	-0.63	-0.61

Scheme 4. Structures and biological profiles of previously identified antileishmanial hit compounds **(A)**, **(B),** and **(C)**.

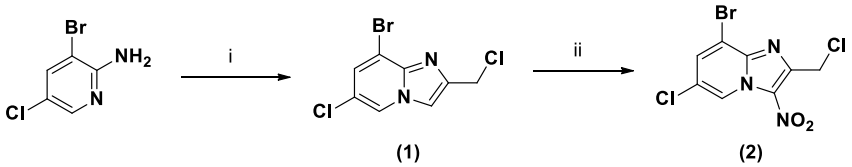

Scheme 5. Synthesis of compounds (1) and (2). Reagents and conditions: (i) 1,3-Dichloroacetone 1.1 equiv, EtOH, reflux, 96 h, 60 %. (ii) HNO_3 65 % 6 equiv, H_2SO_4, 0 °C → RT, 3 h, 60 %.

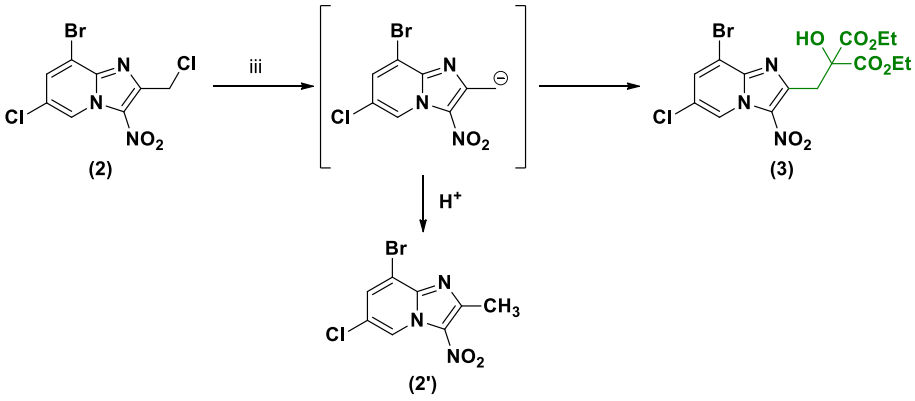

Scheme 6. Synthesis of compound **(3)** and by-product **(2′)**. Reagents and conditions: (iii) Diethyl oxomalonate 3 equiv, TDAE 1 equiv, DMF, N_2, -20 °C, 1 h → RT, 2 h, 45 %.

intermediate at position 2, nor its subsequent addition to an electrophile. The proper progression of the reaction was assessed by the visual formation of a colored charge-transfer complex upon addition of TDAE, and by the detection of traces of a 2-methylated by-product **(2′)** resulting from the reprotonation of the carbanion [18,19]. The presence of by-product **(2')** was confirmed by comparison of its ^{1}H NMR and LCMS data with those previously reported [13].

To modulate the position 2 of the 3-nitroimidazo[1,2-*a*]pyridine with significant chemical diversity, the TDAE methodology was subsequently applied to *N*-tosylbenzylimine derivatives. These electrophiles, which can be readily obtained from the corresponding benzaldehydes, permit a broad array of substituents [20]. The TDAE reaction between intermediate **(2)** and the appropriate *N*-tosylbenzylimine derivative to produce compound **(4a)** was optimized by evaluating several reaction parameters, including solvent, temperature and reaction time (Scheme 7). The optimal conditions for this reaction were 2-methyltetrahydrofuran as solvent, a reaction temperature of −20 °C, and a duration of 30 min, affording compound **(4a)** in 63 % yield.

Applying this newly optimized synthetic route, a series of 11 compounds **(4a–k)** was synthesized from various *N*-tosylbenzylimine derivatives substituted at positions 2, 3, or 4 with different substituents (Scheme 8).

To ascertain the mechanism of action associated with the reduction of the nitro group by parasitic nitroreductases, and consequently confirm the essential nature of the nitro group at position 3, compound **(5)** was synthesized. This compound is analogous to the most promising compound in the initial series **(4h)**, but with an amine group at position 3 (Scheme 9). Compound **(4h)** was reduced using iron powder under conditions that had already been optimized in our laboratory [21].

To approach the chemical structures of the previously identified hits

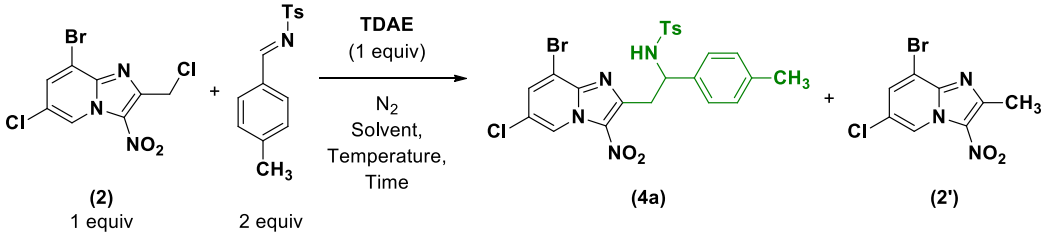

Solvent	Temperature	Time	Yield
Tetrahydrofuran	-20 °C	30 min	52%
Tetrahydrofuran	-20 °C	15 min	22%
Tetrahydrofuran	-20 °C	60 min	22%
Dimethylformamide	-20 °C	30 min	11%
Dimethylformamide	-20 °C, then RT	1 h, then 2 h	0%
2-Methyltetrahydrofuran	**-20 °C**	**30 min**	**63%**

Scheme 7. Optimization of the TDAE reaction between intermediate **(2)** and 4-methyl-*N*-tosylbenzylimine.

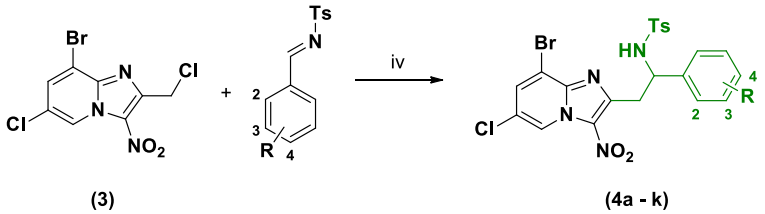

(3) (4a - k)

Compound	(4a)	(4b)	(4c)	(4d)	(4e)	(4f)	(4g)	(4h)	(4i)	(4j)	(4k)
R	4-Me	4-H	4-Et	4-OMe	4-F	4-CF_3	4-Cl	3-Cl	2-Cl	4-Br	4-CN
Yield	63%	76%	45%	54%	67%	50%	30%	51%	40%	55%	40%

Scheme 8. Synthesis of compounds **(4a–k)**. Reagents and conditions: (iv) Appropriate *N*-tosylbenzylimines 2 equiv, TDAE 1 equiv, 2-methyltetrahydrofuran, N_2, -20 °C, 30 min, 30–76 %.

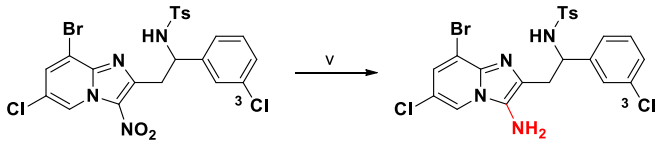

(4h) (5)

Scheme 9. Synthesis of compound **(5)**. Reagents and conditions: (v) Fe 10 equiv, AcOH, reflux, 30 min, 20 %.

(B) and **(C)**, which showed good antiparasitic activities and favorable pharmacokinetic and physicochemical profiles, a modulation at position 8 was performed on the most promising derivatives of the newly synthesized series.

A nucleophilic aromatic substitution was carried out to introduce a *para*-chlorothiophenol moiety at position 8. This reaction had previously been optimized by our team to synthesize hit **(B)** [14]. The same conditions were applied without further optimization and led to the synthesis of five novel compounds **(6a-e)** in good yield, except for **(6c)** (Scheme 10).

Subsequently, sulfur oxidation was performed at position 8 of compound **(6b)** to further study the structure-activity relationships of these compounds. These oxidations were performed using *m*-CPBA under two distinct sets of conditions previously described for hit **(B)** [22]. Given their simplicity and reproducibility, these reactions were conducted without further optimization, resulting in the synthesis of two additional compounds: a derivative bearing a sulfoxide group **(7)** and a derivative bearing a sulfone group **(8)** (Scheme 11).

Concurrently, a Suzuki-Miyaura cross-coupling reaction was employed to introduce a 4-pyridinyl group at position 8. This methodology had previously been optimized by our team to synthesize hit **(C)** [15]. Given the effectiveness of this reaction, further optimization was deemed unnecessary. Consequently, five novel compounds **(9a-e)** were synthesized in moderate yields (Scheme 12).

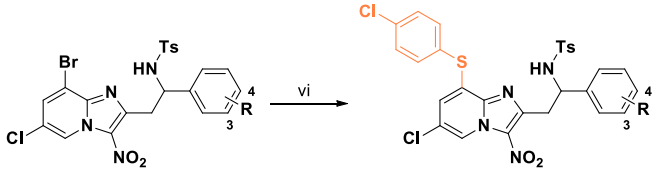

(4a - k) (6a - e)

Compound	(6a)	(6b)	(6c)	(6d)	(6e)
R	4-F	4-Cl	3-Cl	4-Br	4-CN
Yield	72%	81%	20%	57%	74%

Scheme 10. Synthesis of compounds **(6a–e)**. Reagents and conditions: (vi) 4-Chlorothiophenol 2 equiv, NaH 60 % 2 equiv, DMSO, N_2, RT, 15 h, 20–81 %.

2.2. Biological assays

The 25 newly synthesized compounds were evaluated for their *in vitro* antileishmanial activity against the axenic amastigote form of *Leishmania infantum* (Table 1). Their cytotoxicity was simultaneously assessed on THP1-derived macrophages, allowing the determination of the selectivity index (SI). SI was calculated as the ratio CC_{50} (THP1)/IC_{50} (*L. infantum* axe. ama). For a chemical variety of compounds, redox potentials (E_0) of the nitro group were measured using cyclic voltammetry, and the values were corrected versus Normal Hydrogen Electrode (NHE).

Among the most active and selective compounds in the axenic model **(4g)**, **(4h)**, and **(4j)** all displayed submicromolar potency combined with low cytotoxicity. Although compound **(4j)** exhibited the lowest IC_{50} value within the series, it showed poor apparent solubility during preliminary biological evaluation, limiting its interest for further evaluation (formal solubility determination was not performed). For this reason, only compounds **(4g)** and **(4h)** were evaluated against the intramacrophagic amastigote form or *L. infantum*. Selectivity indices were again calculated using the same cytotoxicity reference.

To gain mechanistic insight into the role of the nitro group in bioactivity, a selection of structurally diverse compounds was analyzed using cyclic voltammetry to determine their reduction potential (E_0). This electrochemical parameter correlates with the likelihood of nitro group bioreduction by parasite-specific type I nitroreductases, a key step in the activation of many nitroaromatic prodrugs.

As an initial evaluation, compound **(3)**, obtained with the diethyloxomalonate, was tested for cytotoxicity and *in vitro* antileishmanial activity. However, it displayed a poor profile, with CC_{50} = 23.3 μM on THP1 cells and IC_{50} = 14.25 μM against *L. infantum* axenic amastigotes, resulting in a low selectivity index (SI = 1.6).

The initial series of compounds, featuring a bromine atom at position 8 **(4a–k)**, demonstrated good *in vitro* antileishmanial activity and low cytotoxicity, with selectivity indices greater than 10, thereby qualifying them as potential antileishmanial hits.

Notably, six derivatives exhibited submicromolar IC_{50} values against axenic amastigotes regardless of the electron-donating or -withdrawing properties of the phenyl substituent or its position (para or ortho): **(4c)** (4-ethyl), **(4f)** (4-trifluoromethyl), **(4g)** (4-chloro), **(4h)** (3-chloro), **(4j)** (4-bromo), and **(4k)** (4-cyano). This distribution suggests that the antileishmanial activity is not primarily governed by the electronic nature of the substituent, but rather by steric and hydrophobic contributions. In particular, halogenated derivatives showed consistently strong activity. Among them, compounds **(4g)**, **(4h)**, and **(4j)** combined high antiparasitic activity and low cytotoxicity, resulting in SI exceeding 100.

Although compound **(4j)** displayed excellent potency, poor aqueous solubility was observed during biological evaluation, which limited its potential for additional evaluation.

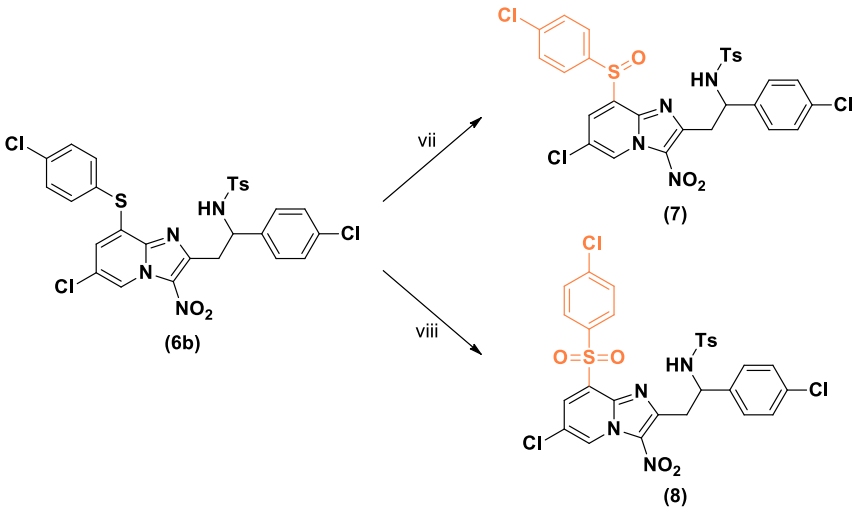

Scheme 11. Synthesis of compounds **(7)** and **(8)**. Reagents and conditions: (vii) *m*-CPBA 1 equiv, dichloromethane, 0 °C, 3 h, 63 %; (viii) *m*-CPBA 2 equiv, DCM, RT, 24 h, 21 %.

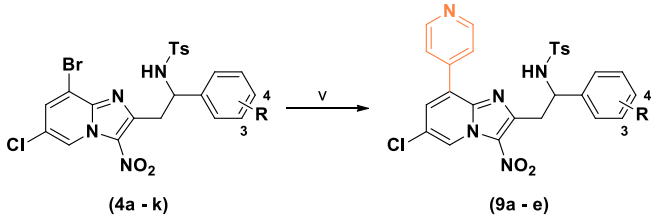

Compound	(9a)	(9b)	(9c)	(9d)	(9e)
R	4-F	4-Cl	3-Cl	4-Br	4-CN
Yield	40%	44%	60%	36%	25%

Scheme 12. Synthesis of compounds **(9a–e)**. Reagents and conditions: (v) 4-Pyridinylboronic acid 1.5 equiv, $Pd(dppf)Cl_2$ 0.1 equiv, K_2CO_3 5 equiv, THF, N_2, 120 °C, MW, 1–2 h, 25–60 %.

Compounds **(4g)** and **(4h)** were further evaluated against the intramacrophagic amastigote form of *L. infantum* to confirm their activity. Both compounds displayed remarkable potency, with **(4g)** exhibiting a modest decrease in activity (IC_{50} = 0.82 μM), and **(4h)** showing no loss of activity (IC_{50} = 0.35 μM). These results surpass those of previously reported hits **(A)**, **(B),** and **(C)** and reference drugs miltefosine and amphotericin B.

Moreover, compound **(4h)** outperforms the activity of the reference drugs miltefosine and amphotericin B, while exhibiting no detectable cytotoxicity in THP1 cells (CC_{50} > 100 μM). Taken together, these data support the selection of compound **(4h)** as a new hit candidate in the 3-nitroimidazo[1,2-*a*]pyridine series. Its selective antileishmanial profile warrants further investigation.

Surprisingly, reduction of the nitro group at position 3 to the corresponding 3-amino analogue **(5)** still resulted in significant antileishmanial activity against the axenic amastigote form (IC_{50} = 2.77 ± 0.14 μM). Although less potent than the parent compound **(4h)**,this finding deviates from previous observations reported for 3-aminoimidazo[1,2-*a*]pyridines, which generally show little or no activity in the absence of nitro-dependent bioactivation by parasite nitroreductases [23,24].

Non-nitrated scaffolds of this family have been described as inhibitors of parasitic and human kinases, including imidazo[1,2-*a*]pyridine derivatives [25]. The residual activity of compound 5 may therefore arise from a nitro-independent mechanism, although this hypothesis requires dedicated investigation.

To further characterize hit **(4h)**, a set of complementary studies was conducted. Its aqueous solubility was determined to be < 1 μM, which may represent a limiting factor for further pharmacokinetic development. The reduction potential (E_0 = −0.60 V) of its nitro group was also only slightly changed compared to previously reported hits (−0.61 to −0.65 V), suggesting that replacing the sulfone group with a carbon chain, together with the *N*-tosyl and benzylic moieties, does not significantly affect the reduction properties of the scaffold. A similar trend was observed for analogues diversified at position 8 which consistently displayed E_0 values between −0.62 and −0.64 V.

The second series of compounds **(6a–e)**, featuring a *para*-chlorothiophenol group at position 8 introduced via an S_NAr reaction, also exhibited good antileishmanial activity and no detectable cytotoxicity on THP1 cells. They displayed SI > 10, ranking compounds **(6a-e)** as potential antileishmanial hits.

Although none of the compounds reached submicromolar IC_{50} values, their activity remained significant. Overall, the *para*-chlorothiophenol-substituted analogues exhibited significantly reduced activity compared to their corresponding 8-brominated counterparts **(4a-k)**, despite maintaining favorable selectivity profiles.

The sulfoxide derivative **(7)** demonstrated a similar activity profile to that of its parent thioether **(6b)** (IC_{50} = 6.93 μM) and no observed cytotoxicity. However, further oxidation of the sulfone resulted in a decrease in antileishmanial activity (IC_{50} = 10.32 μM) for compound **(8)** without cytotoxicity.

These results are consistent with previous observations made on the earlier hit **(B)**, where sulfur oxidation similarly led to reduced potency. Although the sulfoxide derivative retains antileishmanial activity, the progressive loss of activity observed upon oxidation suggests that thiophenol oxidation could represent a metabolic liability, potentially compromising *in vivo* activity.

A third series of five compounds **(9a–e)**, bearing a 4-pyridinyl group at position 8, was introduced via Suzuki–Miyaura cross-coupling reactions and exhibited low cytotoxicity (CC_{50} > 45 μM). However, their antileishmanial activity was considerably diminished, with IC_{50} values ranging from 15.19 μM for compound **(9a)** to > 100 μM for compound **(9b)**.

This modulation was initially explored based on the encouraging profile of hit **(C)**, but no compound of series **(9a-e)** displayed SI > 10, the threshold generally considered for hit validation. Taken together, these results suggest that the introduction of a 4-pyridinyl group at position 8 does not represent an effective strategy to enhance activity within this scaffold and does not warrant further development.

Table 1
In vitro evaluation of compounds **(4a-k)**, **(5)**, **(6a-e)**, **(7)**, **(8),** and **(9a-e)** on the human leukemia monocytic THP1 cell lines, *L. infantum* axenic amastigote form and intramacrophagic amastigote form. Redox potentials (E_0) of the nitro group were measured using cyclic voltammetry and corrected *versus* Normal Hydrogen Electrode (NHE).

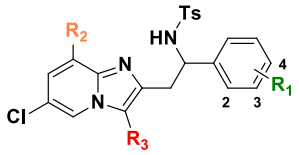

N°	R_1	R_2	R_3	CC_{50} THP1 (μM)	IC_{50} *L. infantum* axe. ama. (μM)	SI THP1/*L. infantum* axe. ama.	IC_{50} *L. infantum* intra. ama. (μM)	SI THP1/*L. infantum* intra. ama.	E_0 (V)
(3)				23.3 ± 1.3	14.25 ± 1.31	1.6	–	–	–
(4a)	4-Me	Br	NO_2	29.8 ± 2.5	1.92 ± 0.37	15.5	–	–	–
(4b)	H	Br	NO_2	100.0 ± 0	1.92 ± 0.33	52.1	–	–	–
(4c)	4-Et	Br	NO_2	22.9 ± 2.2	0.52 ± 0.20	44.0	–	–	–
(4d)	4-OMe	Br	NO_2	>100	1.74 ± 0.17	>57.5	–	–	–
(4e)	4-F	Br	NO_2	100.0 ± 0.0	1.27 ± 0.31	78.7	–	–	–
(4f)	4-CF_3	Br	NO_2	25.6 ± 0.4	0.51 ± 0.11	50.2	–	–	–
(4g)	4-Cl	Br	NO_2	59.6 ± 2.5	0.35 ± 0.19	170.3	0.82 ± 0.04	73	–
(4h)	3-Cl	Br	NO_2	>100	0.42 ± 0.04	>238.1	0.35 ± 0.05	>286	−0.60
(4i)	2-Cl	Br	NO_2	39.0 ± 3.4	2.11 ± 0.49	18.5	–	–	–
(4j)	4-Br	Br	NO_2	>100	0.33 ± 0.11	>303.0	–	–	–
(4k)	4-CN	Br	NO_2	40.8 ± 4.1	0.47 ± 0.20	86.9	–	–	–
(5)	3-Cl	Br	NH_2	22.0 ± 1.3	2.77 ± 0,14	8.0	–	–	–
(6a)	4-F	4-Cl-Ph-S	NO_2	>100	2.69 ± 0.08	>37.13	–	–	−0.63
(6b)	4-Cl	4-Cl-Ph-S	NO_2	>100	6.67 ± 1.58	>14.99	–	–	−0.63
(6c)	3-Cl	4-Cl-Ph-S	NO_2	>100	6.29 ± 1.60	>15.89	–	–	−0.62
(6d)	4-Br	4-Cl-Ph-S	NO_2	>100	3.91 ± 0.96	>25.55	–	–	–
(6e)	4-CN	4-Cl-Ph-S	NO_2	>100	1.25 ± 0.14	>80.00	–	–	–
(7)	4-Cl	4-Cl-Ph-SO	NO_2	>100	6.93 ± 0.75	>14.43	–	–	–
(8)	4-Cl	4-Cl-Ph-SO_2	NO_2	>100	10.32 ± 1.70	>9.69	–	–	–
(9a)	4-F	4-pyridinyl	NO_2	45.8 ± 3.3	15.19 ± 1.99	3.01	–	–	–
(9b)	4-Cl	4-pyridinyl	NO_2	>100	>100	–	–	–	–
(9c)	3-Cl	4-pyridinyl	NO_2	>100	22.57 ± 3.96	>4.43	–	–	−0.64
(9d)	4-Br	4-pyridinyl	NO_2	>100	19.73 ± 4.34	>5.07	–	–	–
(9e)	4-CN	4-pyridinyl	NO_2	>100	43.10 ± 5.80	>2.32	–	–	–
Hit (A)				>100	16.4 ± 0.2	>6.1	2.1 ± 0.1	>47.6	−0.65
Hit **(B)**				>62.5[a]	1.7 ± 0.3	>36.8	3.2 ± 0.1	>19.5	−0.63
Hit **(C)**				>100[a]	14.0 ± 0.9	>7.1	3.7 ± 0.4	>27.0	−0.61
Amphotericin B[b]				5.3 ± 0.3	0.06 ± 0.02	88.4	0.06 ± 0.02	88.3	–
Miltefosine[b]				28.3	0.28 ± 0.01	101.0	0.40 ± 0.14	70.8	–
Doxorubicin[c]				2.4 ± 0.4	–	–	–	–	–

[a] The IC_{50} or CC_{50} value was not reached at the highest tested concentration.
[b] Amphotericin B and miltefosine were used as antileishmanial reference drugs.
[c] Doxorubicin was used as a cytotoxic reference drug.

Overall, modulation at position 2 using the TDAE strategy with *N*-tosylbenzylimine derivatives enabled the synthesis of several new promising antileishmanial candidates, even without improving the redox potential of the nitro group (E_0).

The most potent compounds belong to the 8-brominated series **(4a–k)**, although the *para*-chlorothiophenol derivatives **(6a–e)** and the sulfoxide analogue **(7)** also demonstrated interesting activity profiles.

Compounds **(4g)**, **(4h)**, and **(4j)**, which bear a bromine atom at position 8 and, respectively, a 4-chloro, 3-chloro, and 4-bromo substitution on the benzyl ring at position 2, are the most potent derivatives, with an SI > 100.

Compound **(4h)** also exhibited robust antileishmanial activity against the intramacrophagic amastigote form, with an IC_{50} of 0.35 μM and an SI > 286, underscoring its significant potential. However, its low aqueous solubility remains a major limitation.

3. Conclusion

In this study, we present the successful application of the TDAE methodology with *N*-tosylbenzylimines to access 3-nitroimidazo[1,2-*a*] pyridine derivatives functionalized at position 2. This synthetic approach was optimized and exploited to access a library of 25 new compounds through further diversification at position 8 via S_NAr and Suzuki-Miyaura cross-coupling reactions.

Among these novel compounds, the initial 8-brominated derivatives **(4a–k)** exhibited the most promising results, with six compounds demonstrating submicromolar IC_{50} values against axenic *L. infantum* amastigotes. Conversely, substitutions at position 8 with a 4-pyridinyl group or a *para*-chlorothiophenol group resulted in diminished antileishmanial activity, indicating that further development was not promising.

Compound **(4h)** demonstrated outstanding activity, exhibiting an

IC_{50} of 0.35 μM against the intramacrophagic amastigote form, with no observed cytotoxicity on THP1 cells. These results significantly surpass those of our previously reported hits and approach the *in vitro* activity of reference drugs. Notably, its 3-amino analogue **(5)** retained *in vitro* antileishmanial activity, thereby supporting the hypothesis that additional, nitro-independent mechanisms of action may also be involved in this scaffold.

To further explore its potential, compound **(4h)** underwent additional studies, including electrochemical measurements and aqueous solubility assays. The reduction potential ($E_0 = -0.60$ V) of its nitro group was only slightly shifted compared to previously reported hits confirming that this modulation at position 2 had limited impact on the nitro group reduction potential. Nevertheless, its solubility was found to be very low (<1 μM), which may compromise other early DMPK parameters and limit *in vivo* applicability.

The enhancement of the solubility of compound **(4h)** without compromising its antiparasitic activity, and the investigation of its possible dual mechanism of action, remain pivotal challenges for further development. The *N*-tosyl group at position 2 of the compound has been shown to act as a good leaving group; therefore, its reduction could potentially open a new synthetic pathway to improve the DMPK properties. Although this reduction has not been previously reported for this scaffold, it could represent a promising direction for future optimization.

4. Materials and methods

4.1. Chemistry

4.1.1. General informations

Reagents were purchased from Sigma-Aldrich (Saint-Louis, MO, USA), Fischer Scientific (Pittsburgh, PA, USA) or Fluorochem (Hadfield, UK) and used without further purification. Reaction monitoring was performed using aluminium TLC plates (5 cm × 10 cm) coated with silica gel Xtra SIL G UV254 ALUGRAM® (Macherey-Nagel, Düren, Nordrhein-Westfalen, Germany) in an appropriate eluent. Visualization was performed with ultraviolet light (254 nm). Melting points were determined on a Stuart SMP3 melting point apparatus (Barloworld, Sandton, South Africa) and were uncorrected. HRMS spectra (ESI) were recorded on a SYNAPT G2 HDMS (Waters, Milford, MA, USA) at the Faculté des Sciences de Saint-Jérôme (Marseille, France). NMR spectra were recorded on a Bruker Avance NEO 400 MHz NanoBay spectrometer (Bruker, Billerica, MA, USA) at the Faculté de Pharmacie of Marseille (France) (^{1}H NMR: reference $CDCl_3$ $\delta = 7.26$ ppm, reference DMSO-d_6 $\delta = 2.50$ ppm and ^{13}C NMR: reference $CDCl_3$ $\delta = 77.16$ ppm, reference DMSO-d_6 $\delta = 39.520$ ppm). The following adsorbent was used for column chromatography: silica gel 60 (Merck KGaA, Darmstadt, Germany, particle size 0.063–0.200 mm, 70–230 mesh ASTM). Flash-chromatography was performed using a puriFlash® 5.020 (Interchim, Montluçon, France), with a silica column (IR-50SI) of a size adapted to the crude sample load. The data were processed with InterSoft X. The purity determination of synthesized compounds was checked by LC/MS analyses, which were realized at the Faculté de Pharmacie of Marseille with a Thermo Scientific Vanquish® (Dionex Softron GmbH, Part of Thermo Fisher Scientific, Germering, Germany) coupled using a single quadrupole mass spectrometer Thermo Scientific ISQ EC®. The purity of all the synthesized compounds was >95 %, except for compounds **(4i)**, **(9e)**, **(6e)**, and **(7)** for which the purity was >90 %. The LC/MS data were processed with Chromeleon 7. The RP-HPLC column is a Thermo Hypersil Gold® 50 × 2.1 mm (C18 bounded), with particles of a diameter of 1.9 mm. The volume of the sample injected into the column was 5 μL. Column temperature was 30 °C. Chromatographic analysis, total duration of 10 min, was on the gradient of the following solvents: $t = 0$ min, methanol/water 5:95; $0 < t < 5$ min, linear increase in the proportion of methanol to a methanol/water ratio of 100:0; $5 < t < 7$ min, methanol/water 100:0; $t = 7$ min, return to a methanol/water ratio of 5:95; $7 < t < 10$ min, methanol/water 5:95. The water and methanol used was buffered with 0.1 % formic acid. The flow rate of the mobile phase was 0.4 mL/min. The retention times (t_R) of the molecules analyzed were indicated in min. Optimized mass spectrometric temperature (vaporizer, 350 °C; ion transfer tube, 300 °C) and gas pressure (sheath gas pressure, 60 psig; auxiliary gas pressure, 6 psig; sweep gas pressure, 0.5 psig) were used.

4.1.2. Preparation of diethyl 2-[(8-bromo-6-chloro-3-nitroimidazo[1,2-a]pyridin-2-yl)methyl]-2-hydroxymalonate (3)

To a solution of 8-Bromo-6-chloro-2-chloromethyl-3-nitroimidazo[1,2-*a*]pyridine **(2)** (200 mg, 0.62 mmol, 1 equiv) in dimethylformamide (10 mL) at −20 °C, diethyl oxomalonate was added (322 mg, 1.85 mmol, 3 equiv). Then, tetrakis(dimethylamino)ethylene (144 μL, 0.62 mmol, 1 equiv) was added under an inert atmosphere, and the reaction mixture was stirred for 1 h at −20 °C and then warmed up to room temperature for 2 h. The mixture was slowly poured into 100 mL of an ice-brine mixture. The mixture was extracted three times with 70 mL of ethyl acetate, then the organic layer was washed four times with 100 mL of brine, then dried over anhydrous Na_2SO_4, filtered, and evaporated. Compound **(3)** was obtained after purification by chromatography on silica gel (eluent: dichloromethane-ethyl acetate 99:1) as a pale yellow solid in 45 % yield (129 mg, 0.28 mmol).

mp 115 °C. ^{1}H NMR (400 MHz, DMSO-d_6) δ 9.35 (d, $J = 1.8$ Hz, 1H), 8.38 (d, $J = 1.8$ Hz, 1H), 6.36 (s, 1H), 4.30–4.16 (m, 4H), 3.87 (s, 2H), 1.23 (t, $J = 7.1$ Hz, 6H).^{13}C NMR (101 MHz, DMSO-d_6) δ 169.4, 147.3, 140.3, 133.7, 132.2, 125.6, 125.3, 122.9, 111.6, 78.3, 61.6 (2C), 35.1, 13.9 (2C). LC/MS ESI + t_R 6.573, *(m/z)* $[M+H]^+$ 463.88/465.86/467.91. HRMS (+ESI): 487.9654 $[M+Na]^+$. Calculated for $C_{15}H_{15}BrClN_3O_7Na$: 487.9653.

4.1.3. General procedure for the preparation of N-[2-(8-bromo-6-chloro-3-nitroimidazo[1,2-a]pyridin-2-yl)-1-phenylethyl]-4-methylbenzenesulfonamide derivatives (4a–k)

To a solution of 8-Bromo-6-chloro-2-chloromethyl-3-nitroimidazo[1,2-*a*]pyridine (200 mg, 0.62 mmol, 1 equiv) in 2-methyltetrahydrofuran (20 mL) at −20 °C was added the appropriate (*E*)-*N*-benzylidene-4-methylbenzenesulfonamide (1.24 mmol, 2 equiv). Then, tetrakis(dimethylamino)ethylene (144 μL, 0.62 mmol, 1 equiv) was added under an inert atmosphere, and the reaction mixture was stirred for 30 min at −20 °C.

4.1.3.1. N-[2-(8-bromo-6-chloro-3-nitroimidazo[1,2-a]pyridin-2-yl)-1-(p-tolyl)ethyl]-4-methylbenzenesulfonamide (4a). Starting from (*E*)-4-Methyl-*N*-(4-methylbenzylidene)benzenesulfonamide (339 mg), the mixture was slowly poured into an 100 mL of an ice-water mixture. The mixture was extracted three times with 70 mL of dichloromethane. Then, the organic layer was dried over anhydrous Na_2SO_4, filtered, and evaporated. Compound **(4a)** was obtained after purification by chromatography on silica gel (eluent: dichloromethane-ethyl acetate 98:2) as a pale yellow solid in 63 % yield (220 mg, 0.39 mmol).

mp 183 °C. ^{1}H NMR (400 MHz, $CDCl_3$) δ 9.26 (d, $J = 1.8$ Hz, 1H), 7.90 (d, $J = 1.8$ Hz, 1H), 7.39–7.31 (m, 4H), 7.15 (d, $J = 7.9$ Hz, 2H), 6.84 (d, $J = 7.9$ Hz, 2H), 5.56 (s, 1H), 4.88 (dd, $J = 11.0$, 3.9 Hz, 1H), 3.60 (dd, $J = 14.0$, 3.9 Hz, 1H), 3.53–3.44 (m, 1H), 2.34 (s, 3H), 2.25 (s, 3H). ^{13}C NMR (101 MHz, $CDCl_3$) δ 149.8, 142.7, 140.9, 138.3, 137.7, 137.7, 133.9, 131.1, 129.6 (2C), 128.8 (2C), 126.5 (2C), 126.3 (2C), 124.8, 124.6, 112.7, 56.5, 37.9, 21.6, 21.2. LC/MS ESI + t_R 7.047, *(m/z)* $[M+H]^+$ 563.30/565.27. HRMS (+ESI): 586.9948 $[M+Na]^+$. Calculated for $C_{23}H_{20}BrClN_4O_4SNa$: 586.9949.

4.1.3.2. N-[2-(8-bromo-6-chloro-3-nitroimidazo[1,2-a]pyridin-2-yl)-1-phenylethyl]-4-methylbenzenesulfonamide (4b). Starting from (*E*)-*N*-Benzylidene-4-methylbenzenesulfonamide (322 mg), the mixture was slowly poured into 100 mL of an ice-water mixture. The mixture was extracted three times with 70 mL of dichloromethane. Then, the organic

layer was dried over anhydrous Na_2SO_4, filtered, and evaporated. Compound **(4b)** was obtained after purification by chromatography on silica gel (eluent: cyclohexane-dichloromethane-methanol gradient from 40:60:0 to 0:99.4:0.6) as a beige solid in 76 % yield (259 mg, 0.47 mmol).

mp 190 °C. ^{1}H NMR (400 MHz, $CDCl_3$) δ 9.26 (d, J = 1.9 Hz, 1H), 7.91 (d, J = 1.9 Hz, 1H), 7.46 (d, J = 7.5 Hz, 2H), 7.39–7.32 (m, 4H), 7.29 (d, J = 7.3 Hz, 1H), 6.84 (d, J = 7.8 Hz, 2H), 5.57 (s, 1H), 4.92 (d, J = 10.9 Hz, 1H), 3.62 (dd, J = 14.0, 3.9 Hz, 1H), 3.46 (dd, J = 13.8, 11.2 Hz, 1H), 2.26 (s, 3H). ^{13}C NMR (101 MHz, $CDCl_3$) δ 149.7, 142.7, 141.2, 141.0, 137.6, 133.9, 131.1, 128.9 (2C), 128.8 (2C), 128.0, 126.5 (2C), 126.4 (2C), 124.8, 124.6, 112.8, 56.7, 37.9, 21.6. LC/MS ESI + t_R 6.877, *(m/z)* $[M+H]^+$ 549.27/551.25. HRMS (+ESI): 550.9900 $[M+H]^+$. Calculated for $C_{22}H_{19}BrClN_4O_4S$: 550.9973.

4.1.3.3. N-[2-(8-bromo-6-chloro-3-nitroimidazo[1,2-a]pyridin-2-yl)-1-(4-ethylphenyl)ethyl]-4-methylbenzenesulfonamide (4c). Starting from (*E*)-4-Methyl-*N*-(4-ethylbenzylidene)benzenesulfonamide (382 mg), the mixture was slowly poured into 100 mL of an ice-water mixture. The mixture was extracted three times with 70 mL of dichloromethane, then the organic layer was dried over anhydrous Na_2SO_4, filtered, and evaporated. Compound **(4c)** was obtained after purification by chromatography on silica gel (eluent: cyclohexane-dichloromethane-methanol gradient from 40:60:0 to 0:99.9:0.1) as a beige solid in 45 % yield (161 mg, 0.28 mmol).

mp 157 °C. ^{1}H NMR (400 MHz, $CDCl_3$) δ 9.26 (d, J = 1.8 Hz, 1H), 7.90 (d, J = 1.8 Hz, 1H), 7.39–7.32 (m, 4H), 7.16 (d, J = 8.2 Hz, 2H), 6.83 (d, J = 8.0 Hz, 2H), 5.58 (s, 1H), 4.97–4.84 (m, 1H), 3.60 (dd, J = 14.0, 3.9 Hz, 1H), 3.46 (dd, J = 14.0, 11.1 Hz, 1H), 2.63 (q, J = 7.6 Hz, 2H), 2.25 (s, 3H), 1.23 (t, J = 7.6 Hz, 3H). ^{13}C NMR (101 MHz, $CDCl_3$) δ 149.9, 144.0, 142.6, 140.9, 138.4, 137.7, 133.8, 131.1, 128.8 (2C), 128.4 (2C), 126.5 (2C), 126.3 (2C), 124.8 (2C), 124.6, 112.7, 56.5, 37.9, 28.6, 21.6, 15.7. LC/MS ESI + t_R 7.183, *(m/z)* $[M+H]^+$ 577.33/579.32. HRMS (+ESI): 601.0103 $[M+Na]^+$. Calculated for $C_{24}H_{22}BrClN_4O_4SNa$: 601.0105.

4.1.3.4. N-[2-(8-bromo-6-chloro-3-nitroimidazo[1,2-a]pyridin-2-yl)-1-(4-methoxyphenyl)ethyl]-4-methylbenzenesulfonamide (4d). Starting from (*E*)-4-Methyl-*N*-(4-benzylidene)benzenesulfonamide (359 mg), the mixture was slowly poured into 100 mL of an ice-water mixture. The mixture was extracted three times with 70 mL of dichloromethane. Then, the organic layer was dried over anhydrous Na_2SO_4, filtered, and evaporated. Compound **(4d)** was obtained after purification by chromatography on silica gel (eluent: dichloromethane-methanol gradient from 100:0 to 99:1) as a pale yellow solid in 54 % yield (194 mg, 0.33 mmol).

mp 202 °C. ^{1}H NMR (400 MHz, $CDCl_3$) δ 9.26 (s, 1H), 7.90 (s, 1H), 7.36 (d, J = 6.6 Hz, 4H), 6.91–6.75 (m, 4H), 5.54 (s, 1H), 4.88 (d, J = 9.3 Hz, 1H), 3.80 (s, 3H), 3.63–3.54 (m, 1H), 3.47 (t, J = 12.3 Hz, 1H), 2.26 (s, 3H). ^{13}C NMR (101 MHz, $CDCl_3$) δ 159.3, 149.8, 142.7, 137.7, 133.9, 133.4, 129.9, 128.8 (2C), 127.6 (2C), 126.6, 126.5 (2C), 124.8, 124.6, 114.2 (2C), 112.8, 56.2, 55.5, 37.9, 21.6. LC/MS ESI + t_R 6.873, *(m/z)* $[M+H]^+$ 579.32/581.33. HRMS (+ESI): 581.0084 $[M+H]^+$. Calculated for $C_{23}H_{21}BrClN_4O_5S$: 581.0078.

4.1.3.5. N-[2-(8-bromo-6-chloro-3-nitroimidazo[1,2-a]pyridin-2-yl)-1-(4-fluorophenyl)ethyl]-4-methylbenzenesulfonamide (4e). Starting from (*E*)-4-Methyl-*N*-(4-fluorobenzylidene)benzenesulfonamide (344 mg), the mixture was slowly poured into 100 mL of an ice-water mixture. The mixture was extracted three times with 70 mL of dichloromethane. Then, the organic layer was dried over anhydrous Na_2SO_4, filtered, and evaporated. Compound **(4e)** was obtained after purification by chromatography on silica gel (eluent: dichloromethane-methanol gradient from 100:0 to 99.4:0.6) as a pale beige solid in 67 % yield (236 mg, 0.42 mmol).

mp 186 °C. ^{1}H NMR (400 MHz, $CDCl_3$) δ 9.26 (d, J = 1.8 Hz, 1H), 7.91 (d, J = 1.9 Hz, 1H), 7.44 (dd, J = 8.5, 5.2 Hz, 2H), 7.35 (d, J = 7.9 Hz, 2H), 7.03 (t, J = 8.5 Hz, 2H), 6.85 (d, J = 7.9 Hz, 2H), 5.60 (s, 1H), 4.89 (d, J = 9.3 Hz, 1H), 3.59 (dd, J = 14.1, 3.8 Hz, 1H), 3.42 (dd, J = 14.1, 11.0 Hz, 1H), 2.26 (s, 3H). ^{13}C NMR (101 MHz, $CDCl_3$) δ 162.4 (d, J = 246.4 Hz), 149.4, 142.9, 141.0, 137.5, 137.0 (d, J = 3.4 Hz), 134.0, 129.9, 128.9 (2C), 128.1 (d, J = 8.0 Hz, 2C), 126.5 (2C), 124.8 (2C), 115.8 (d, J = 21.5 Hz, 2C), 112.8, 56.0, 37.9, 21.6. LC/MS ESI + t_R 6.917, *(m/z)* $[M+H]^+$ 567.26/569.26. HRMS (+ESI): 568.9877 $[M+H]^+$. Calculated for $C_{22}H_{18}BrClFN_4O_4S$: 568.9878.

4.1.3.6. N-{2-(8-bromo-6-chloro-3-nitroimidazo[1,2-a]pyridin-2-yl)-1-[4-(trifluoromethyl)phenyl]ethyl}-4-methylbenzenesulfonamide (4f). Starting from (*E*)-4-Methyl-*N*-(4-(trifluoromethyl)benzylidene)benzenesulfonamide (406 mg), the mixture was slowly poured into 100 mL of an ice-water mixture. The mixture was extracted three times with 70 mL of dichloromethane. Then, the organic layer was dried over anhydrous Na_2SO_4, filtered, and evaporated. Compound **(4f)** was obtained after purification by chromatography on silica gel (eluent: dichloromethane-diethyl ether gradient from 100:0 to 98:2) as a white solid in 50 % yield (191 mg, 0.31 mmol).

mp 176 °C. ^{1}H NMR (400 MHz, $CDCl_3$) δ 9.26 (d, J = 1.8 Hz, 1H), 7.93 (d, J = 1.8 Hz, 1H), 7.59 (s, 4H), 7.37–7.31 (m, 2H), 6.84 (d, J = 7.9 Hz, 2H), 5.74 (d, J = 7.0 Hz, 1H), 4.95 (ddd, J = 10.8, 7.0, 3.7 Hz, 1H), 3.63 (dd, J = 14.1, 3.8 Hz, 1H), 3.41 (dd, J = 14.2, 10.9 Hz, 1H), 2.26 (s, 3H). ^{13}C NMR (101 MHz, $CDCl_3$) δ 149.0, 145.0, 143.1, 141.0, 137.3, 134.1, 130.9, 130.2 (q, J = 32.4 Hz), 128.9 (2C), 126.9 (2C), 126.5 (2C), 125.9 (q, J = 3.8 Hz, 2C), 124.9, 124.8, 124.1 (q, J = 272.2 Hz), 112.9, 56.2, 37.6, 21.6. LC/MS ESI + t_R 7.137, *(m/z)* $[M+H]^+$ 617.29/619.29. HRMS (+ESI): 640.9668 $[M+Na]^+$. Calculated for $C_{23}H_{17}BrClF_3N_4O_4SNa$: 640.9666.

4.1.3.7. N-[2-(8-bromo-6-chloro-3-nitroimidazo[1,2-a]pyridin-2-yl)-1-(4-chlorophenyl)ethyl]-4-methylbenzenesulfonamide (4g). Starting from (*E*)-4-Methyl-*N*-(4-chlorobenzylidene)benzenesulfonamide (364 mg), the mixture was slowly poured into 100 mL of an ice-water mixture. The mixture was extracted three times with 70 mL of dichloromethane. Then, the organic layer was dried over anhydrous Na_2SO_4, filtered, and evaporated. Compound **(4g)** was obtained after purification by chromatography on silica gel (eluent: dichloromethane-methanol 99.8:0.2) as a beige solid in 30 % yield (108 mg, 0.19 mmol).

mp 190 °C. ^{1}H NMR (400 MHz, $CDCl_3$) δ 9.26 (d, J = 1.7 Hz, 1H), 7.92 (d, J = 1.8 Hz, 1H), 7.41 (d, J = 8.5 Hz, 2H), 7.35 (d, J = 7.9 Hz, 2H), 7.31 (d, J = 8.5 Hz, 2H), 6.85 (d, J = 7.9 Hz, 2H), 5.69 (d, J = 6.9 Hz, 1H), 4.93–4.83 (m, 1H), 3.59 (dd, J = 14.1, 3.8 Hz, 1H), 3.40 (dd, J = 14.1, 11.0 Hz, 1H), 2.27 (s, 3H). ^{13}C NMR (101 MHz, $CDCl_3$) δ 149.3, 143.0, 141.0, 139.7, 137.4, 134.0, 133.8, 131.0, 129.0 (2C), 128.9 (2C), 127.8 (2C), 126.5 (2C), 124.8, 124.8, 112.8, 56.0, 37.7, 21.6. LC/MS ESI + t_R 7.097, *(m/z)* $[M+H]^+$ 583.32/585.28/587.31. HRMS (+ESI): 606.9405 $[M+Na]^+$. Calculated for $C_{22}H_{17}BrCl_2N_4O_4SNa$: 606.9401.

4.1.3.8. N-[2-(8-bromo-6-chloro-3-nitroimidazo[1,2-a]pyridin-2-yl)-1-(3-chlorophenyl)ethyl]-4-methylbenzenesulfonamide (4h). Starting from (*E*)-4-Methyl-*N*-(3-chlorobenzylidene)benzenesulfonamide (364 mg), the mixture was slowly poured into 100 mL of an ice-water mixture. The mixture was extracted three times with 70 mL of dichloromethane. Then, the organic layer was dried over anhydrous Na_2SO_4, filtered, and evaporated. Compound **(4h)** was obtained after purification by chromatography on silica gel (eluent: dichloromethane) as a white solid in 51 % yield (185 mg, 0.32 mmol).

mp 209 °C. ^{1}H NMR (400 MHz, $CDCl_3$) δ 9.26 (d, J = 1.8 Hz, 1H), 7.92 (d, J = 1.8 Hz, 1H), 7.41 (t, J = 1.9 Hz, 1H), 7.39–7.33 (m, 3H), 7.29 (d, J = 7.9 Hz, 1H), 7.26–7.21 (m, 1H), 6.85 (d, J = 8.0 Hz, 2H), 5.67 (d, J = 7.1 Hz, 1H), 4.88 (ddd, J = 11.0, 7.2, 3.8 Hz, 1H), 3.61 (dd, J = 14.1, 3.8 Hz, 1H), 3.40 (dd, J = 14.1, 11.0 Hz, 1H), 2.26 (s, 3H). ^{13}C

NMR (101 MHz, $CDCl_3$) δ 149.2, 143.1, 143.0, 141.0, 137.3, 134.8, 134.0, 131.0, 130.2, 128.9 (2C), 128.2, 126.8, 126.5 (2C), 124.8, 124.8, 124.6, 112.9, 56.1, 37.7, 21.6. LC/MS ESI + t_R 7.080, *(m/z)* $[M+H]^+$ 583.25/585.24/587.25. HRMS (+ESI): 584.9583 $[M+H]^+$. Calculated for $C_{22}H_{18}BrCl_2N_4O_4S$: 584.9581.

4.1.3.9. N-[2-(8-bromo-6-chloro-3-nitroimidazo[1,2-a]pyridin-2-yl)-1-(2-chlorophenyl)ethyl]-4-methylbenzenesulfonamide (4i). Starting from (*E*)-4-Methyl-*N*-(2-chlorobenzylidene)benzenesulfonamide (364 mg), the mixture was slowly poured into 100 mL of an ice-water mixture. The mixture was extracted three times with 70 mL of dichloromethane. Then, the organic layer was dried over anhydrous Na_2SO_4, filtered, and evaporated. Compound **(4i)** was obtained after purification by chromatography on silica gel (eluent: dichloromethane-methanol gradient from 100:0 to 99:1) as a pale yellow solid in 40 % yield (145 mg, 0.25 mmol).

mp 222 °C. ^{1}H NMR (400 MHz, $CDCl_3$) δ 9.27 (d, J = 1.8 Hz, 1H), 7.91 (d, J = 1.8 Hz, 1H), 7.53 (dd, J = 7.4, 2.1 Hz, 1H), 7.42–7.37 (m, 2H), 7.34 (dd, J = 7.6, 1.7 Hz, 1H), 7.21 (qd, J = 7.3, 1.8 Hz, 2H), 6.89–6.83 (m, 2H), 5.99 (d, J = 7.3 Hz, 1H), 5.25 (ddd, J = 11.1, 7.3, 4.2 Hz, 1H), 3.67 (dd, J = 14.1, 4.2 Hz, 1H), 3.50 (dd, J = 14.1, 10.5 Hz, 1H), 2.27 (s, 3H). ^{13}C NMR (101 MHz, $CDCl_3$) δ 149.0, 142.9, 140.9, 138.4, 137.2, 133.9, 132.3, 131.0, 130.1, 129.2, 128.9 (2C), 128.9, 127.4, 126.6 (2C), 124.7, 124.6, 112.8, 54.4, 35.6, 21.6. LC/MS ESI + t_R 7.017, *(m/z)* $[M+H]^+$ 583.11/585.03/587.08. HRMS (+ESI): 584.9587 $[M+H]^+$. Calculated for $C_{22}H_{18}BrCl_2N_4O_4S$: 584.9581.

4.1.3.10. N-[2-(8-bromo-6-chloro-3-nitroimidazo[1,2-a]pyridin-2-yl)-1-(4-bromophenyl)ethyl]-4-methylbenzenesulfonamide (4j). Starting from (*E*)-4-Methyl-*N*-(4-bromobenzylidene)benzenesulfonamide (419 mg), the mixture was slowly poured into 100 mL of an ice-water mixture. The mixture was extracted three times with 70 mL of dichloromethane, then the organic layer was dried over anhydrous Na_2SO_4, filtered, and evaporated. Compound **(4j)** was obtained after purification by chromatography on silica gel (eluent: dichloromethane-methanol gradient from 100:0 to 99:1) as a pale yellow solid in 55 % yield (214 mg, 0.34 mmol).

mp 198 °C. ^{1}H NMR (400 MHz, $CDCl_3$) δ 9.25 (d, J = 1.7 Hz, 1H), 7.91 (d, J = 1.8 Hz, 1H), 7.48–7.42 (m, 2H), 7.37–7.30 (m, 4H), 6.85 (d, J = 8.0 Hz, 2H), 5.67 (d, J = 7.2 Hz, 1H), 4.90–4.80 (m, 1H), 3.58 (dd, J = 14.1, 3.8 Hz, 1H), 3.40 (dd, J = 14.1, 11.0 Hz, 1H), 2.26 (s, 3H). ^{13}C NMR (101 MHz, $CDCl_3$) δ 149.2, 143.0, 141.0, 140.2, 137.4, 134.0, 132.0 (2C), 131.0, 128.9 (2C), 128.2 (2C), 126.5 (2C), 124.8, 124.7, 121.9, 112.8, 56.1, 37.6, 21.6. LC/MS ESI + t_R 7.130, *(m/z)* $[M+H]^+$ 628.93/630.91. HRMS (+ESI): 628.9078 $[M+H]^+$. Calculated for $C_{22}H_{18}Br_2ClN_4O_4S$: 628.9078.

4.1.3.11. N-[2-(8-bromo-6-chloro-3-nitroimidazo[1,2-a]pyridin-2-yl)-1-(4-cyanophenyl)ethyl]-4-methylbenzenesulfonamide (4k). Starting from (*E*)-4-Methyl-*N*-(4-cyanobenzylidene)benzenesulfonamide (353 mg), the mixture was slowly poured into 100 mL of an ice-water mixture. The mixture was extracted three times with 70 mL of dichloromethane. Then, the organic layer was dried over anhydrous Na_2SO_4, filtered, and evaporated. Compound **(4k)** was obtained after purification by chromatography on silica gel (eluent: dichloromethane-methanol gradient from 100:0 to 99:1) as a dark yellow solid in 40 % yield (143 mg, 0.25 mmol).

mp 235 °C. ^{1}H NMR (400 MHz, $CDCl_3$) δ 9.24 (d, J = 1.8 Hz, 1H), 7.93 (d, J = 1.8 Hz, 1H), 7.71–7.58 (m, 4H), 7.34 (d, J = 8.1 Hz, 2H), 6.84 (d, J = 7.9 Hz, 2H), 5.84 (d, J = 6.8 Hz, 1H), 4.91 (ddd, J = 10.7, 6.9, 3.7 Hz, 1H), 3.61 (dd, J = 14.2, 3.7 Hz, 1H), 3.36 (dd, J = 14.2, 11.0 Hz, 1H), 2.26 (s, 3H). ^{13}C NMR (101 MHz, $CDCl_3$) δ 148.7, 146.4, 143.2, 141.0, 137.1, 134.2, 132.8 (2C), 130.9, 129.0 (2C), 127.3 (2C), 126.5 (2C), 125.0, 124.7, 118.7, 112.9, 112.0, 56.2, 37.4, 21.6. LC/MS ESI + t_R 6.703, *(m/z)* $[M+H]^+$ 574.22/576.21. HRMS (+ESI): 575.9928 $[M+H]^+$. Calculated for $C_{23}H_{18}BrClN_5O_4S$: 575.9925.

4.1.4. Preparation of N-[2-(3-amino-8-bromo-6-chloroimidazo[1,2-a]pyridin-2-yl)-1-(3-chloro-phenyl)ethyl]-4-methylbenzenesulfonamide (5)

To a solution of *N*-[2-(8-Bromo-6-chloro-3-nitroimidazo[1,2-*a*]pyridin-2-yl)-1-(3-chlorophenyl)ethyl]-4-methylbenzenesulfonamide **(4h)** (200 mg, 0.34 mmol, 1 equiv) in acetic acid (30 mL) was added iron powder (192 mg, 3.42 mmol, 10 equiv). The reaction mixture was stirred and heated under reflux for 30 min. The mixture was then filtered through Celite and the solvent was evaporated *in vacuo*. The resulting residue was diluted with 100 mL of H_2O, extracted three times with 70 mL of dichloromethane, and then the organic layer was dried over anhydrous Na_2SO_4, filtered, and evaporated. Compound **(5)** was obtained after purification by chromatography on silica gel (eluent: dichloromethane-ethyl acetate gradient from 1:0 to 8:2) as a brown solid in 20 % yield (38 mg, 0.07 mmol).

mp 170 °C. ^{1}H NMR (400 MHz, $CDCl_3$) δ 7.88 (d, J = 1.8 Hz, 1H), 7.46–7.40 (m, 2H), 7.38 (d, J = 1.8 Hz, 1H), 7.23–7.15 (m, 4H), 6.94 (d, J = 8.0 Hz, 2H), 6.68 (d, J = 5.9 Hz, 1H), 4.70–4.60 (m, 1H), 3.10–2.95 (m, 2H), 2.85 (s, 2H), 2.28 (s, 3H).^{13}C NMR (101 MHz, $CDCl_3$) δ 143.6, 143.0, 137.4, 137.1, 134.4, 129.9, 129.0 (2C), 127.77, 127.1, 126.9, 126.8, 126.8 (2C), 125.2, 125.2, 125.0, 122.4, 119.7, 57.4, 34.2, 21.6. LC/MS ESI + t_R 6.590, *(m/z)* $[M+H]^+$ 553.01/555.07/557.05. HRMS (+ESI): 554.9838 $[M+H]^+$. Calculated for $C_{22}H_{20}BrCl_2N_4O_2S$: 554.9839.

4.1.5. General procedure for the preparation of N-(2-{6-chloro-8-[(4-chlorophenyl)thio]-3-nitroimidazo[1,2-a]pyridin-2-yl}-1-phenylethyl)-4-methylbenzenesulfonamide derivatives (6a–e)

To a solution of sodium hydride 60 % (2 equiv) in dimethylsulfoxide (3 mL) at room temperature, 4-chlorothiophenol (2 equiv) was added. The reaction mixture was sealed, placed under an inert atmosphere, and stirred for 30 min. Then to the reaction mixture was added a solution of the appropriate *N*-[2-(8-Bromo-6-chloro-3-nitroimidazo[1,2-*a*]pyridin-2-yl)-1-phenylethyl]-4-methyl-benzenesulfonamide (200 mg, 1 equiv) in DMSO (6 mL). The reaction mixture was sealed, placed under an inert atmosphere, and stirred overnight.

4.1.5.1. N-(2-{6-chloro-8-[(4-chlorophenyl)thio]-3-nitroimidazo[1,2-a]pyridin-2-yl}-1-(4-fluorophenyl)-ethyl)-4-methylbenzenesulfonamide (6a). Starting from NaH 60 % (28 mg, 0.70 mmol), 4-chlorothiophenol (102 mg, 0.70 mmol) and *N*-[2-(8-Bromo-6-chloro-3-nitroimidazo[1,2-*a*]pyridin-2-yl)-1-(4-fluorophenyl)ethyl]-4-ethylbenzenesulfonamide **(4e)** (0.35 mmol), the mixture was slowly poured into 100 mL of an ice-brine mixture and precipitated. The solid was collected by filtration and dried under reduced pressure. Compound **(6a)** was obtained after purification by chromatography on silica gel (eluent: dichloromethane-methanol gradient from 100:0 to 99:1) as a yellow solid in 72 % yield (129 mg, 0.25 mmol).

mp 183 °C. ^{1}H NMR (400 MHz, DMSO-d_6) δ 9.01 (d, J = 1.8 Hz, 1H), 8.67 (d, J = 9.4 Hz, 1H), 7.76–7.64 (m, 4H), 7.49–7.41 (m, 2H), 7.27–7.21 (m, 2H), 7.20–7.10 (m, 2H), 6.98 (d, J = 1.8 Hz, 1H), 6.93–6.81 (m, 2H), 4.90–4.76 (m, 1H), 3.42–3.33 (m, 2H), 2.13 (s, 3H). ^{13}C NMR (101 MHz, DMSO-d_6) δ 148.9, 140.5 (d, J = 227.5 Hz), 138.7 (d, J = 2.9 Hz), 138.4, 136.6 (2C), 135.4, 130.6 (2C), 130.4, 129.9, 129.3, 128.5 (2C), 128.2 (d, J = 8.0 Hz, 2C), 127.0, 126.7, 125.6, 125.5 (2C), 123.6, 122.7, 115.1 (d, J = 21.2 Hz, 2C), 55.0, 38.0, 20.9. LC/MS ESI + t_R 7.487, *(m/z)* $[M+H]^+$ 631.18/633.24. HRMS (+ESI): 631.0436 $[M+H]^+$. Calculated for $C_{28}H_{22}Cl_2FN_4O_4S_2$: 631.0438.

4.1.5.2. N-(2-{6-chloro-8-[(4-chlorophenyl)thio]-3-nitroimidazo[1,2-a]pyridin-2-yl}-1-(4-chlorophenyl)ethyl)-4-methylbenzenesulfonamide (6b). Starting from NaH 60 % (27 mg, 0.68 mmol), 4-chlorothiophenol (99 mg, 0.68 mmol) and *N*-[2-(8-Bromo-6-chloro-3-nitroimidazo[1,2-*a*]pyridin-2-yl)-1-(4-chlorophenyl)ethyl]-4-ethylbenzenesulfonamide

(4g) (0.34 mmol), the mixture was slowly poured into 100 mL of an ice-brine mixture and precipitated. The solid was collected by filtration and dried under reduced pressure. Compound **(6b)** was obtained after purification by chromatography on silica gel (eluent: cyclohexane-dichloromethane gradient from 1:0 to 0:1) as a yellow solid in 81 % yield (178 mg, 0.27 mmol).

mp 186 °C. ^{1}H NMR (400 MHz, DMSO-d_6) δ 9.02 (d, J = 1.8 Hz, 1H), 8.70 (d, J = 9.4 Hz, 1H), 7.76–7.64 (m, 4H), 7.45–7.36 (m, 4H), 7.26–7.21 (m, 2H), 6.99 (d, J = 1.8 Hz, 1H), 6.91 (d, J = 8.1 Hz, 2H), 4.87–4.77 (m, 1H), 3.40–3.33 (m, 2H), 2.14 (s, 3H). ^{13}C NMR (101 MHz, DMSO-d_6) δ 148.8, 141.7, 141.3, 139.3, 138.3, 136.5 (2C), 135.4, 131.8, 130.6 (2C), 130.4, 129.8, 128.5 (2C), 128.3 (2C), 128.2 (2C), 127.0, 126.8, 125.5 (2C), 123.6, 122.7, 55.1, 37.7, 20.9. LC/MS ESI + t_R 7.630, *(m/z)* $[M+H]^+$ 647.20/649.13/651.12. HRMS (+ESI): 649.0124 $[M+H]^+$. Calculated for $C_{28}H_{22}Cl_3N_4O_4S_2$: 649.0117.

4.1.5.3. N-(2-{6-chloro-8-[(4-chlorophenyl)thio]-3-nitroimidazo[1,2-a] pyridin-2-yl}-1-(3-chlorophenyl)ethyl)-4-methylbenzenesulfonamide (6c). Starting from NaH 60 % (27 mg, 0.68 mmol), 4-chlorothiophenol (99 mg, 0.68 mmol) and *N*-[2-(8-Bromo-6-chloro-3-nitroimidazo[1,2-*a*] pyridin-2-yl)-1-(3-chlorophenyl)ethyl]-4-methylbenzenesulfonamide **(4h)** (0.34 mmol), the mixture was slowly poured into 100 mL of an ice-brine mixture and was extracted three times with 70 mL of ethyl acetate. Then, the organic layer was washed four times with 100 mL of brine, then dried over anhydrous Na_2SO_4, filtered, and evaporated. Compound **(6c)** was obtained after purification by chromatography on silica gel (eluent: dichloromethane-ethyl acetate gradient from 100:0 to 99:1) as a yellow solid in 20 % yield (44 mg, 0.068 mmol).

mp 182 °C. ^{1}H NMR (400 MHz, DMSO-d_6) δ 9.02 (d, J = 1.8 Hz, 1H), 8.71 (d, J = 9.5 Hz, 1H), 7.77–7.70 (m, 2H), 7.69–7.64 (m, 2H), 7.49–7.42 (m, 1H), 7.39–7.35 (m, 2H), 7.35–7.29 (m, 1H), 7.26–7.21 (m, 2H), 6.99 (d, J = 1.8 Hz, 1H), 6.93–6.87 (m, 2H), 4.87–4.77 (m, 1H), 3.41–3.33 (m, 2H), 2.14 (s, 3H). ^{13}C NMR (101 MHz, DMSO-d_6) δ 148.7, 144.7, 141.7, 139.3, 138.2, 136.6 (2C), 135.4, 133.1, 130.6 (2C), 130.4, 130.3, 129.9, 128.5 (2C), 127.2, 126.9, 126.7, 126.2, 125.5 (2C), 125.0, 123.6, 122.6, 55.2, 37.7, 20.9. LC/MS ESI + t_R 7.610. HRMS (+ESI): 649.0114 [M+H]+. Calculated for $C_{28}H_{22}Cl_3N_4O_4S_2$: 649.0117.

4.1.5.4. N-(1-(4-Bromophenyl)-2-{6-chloro-8-[(4-chlorophenyl)thio]-3-nitroimidazo[1,2-a]pyridin-2-yl}ethyl)-4-methylbenzenesulfonamide (6d). Starting from NaH 60 % (25 mg, 0.64 mmol), 4-chlorothiophenol (92 mg, 0.64 mg) and *N*-[2-(8-Bromo-6-chloro-3-nitroimidazo[1,2-*a*]pyridin-2-yl)-1-(4-bromophenyl)ethyl]-4-methylbenzenesulfonamide **(4j)** (0.32 mmol), the mixture was slowly poured into 100 mL of an ice-water mixture and precipitated. The solid was collected by filtration and dried under reduced pressure. Compound **(6d)** was obtained after purification by chromatography on silica gel (eluent: cyclohexane-dichloromethane gradient from 5:5 to 0:1) as a pale yellow solid in 57 % yield (126 mg, 0.18 mmol).

mp 195 °C. ^{1}H NMR (400 MHz, DMSO-d_6) δ 9.02 (d, J = 1.8 Hz, 1H), 8.69 (d, J = 9.4 Hz, 1H), 7.77–7.69 (m, 2H), 7.70–7.62 (m, 2H), 7.55–7.48 (m, 2H), 7.39–7.32 (m, 2H), 7.27–7.20 (m, 2H), 6.99 (d, J = 1.9 Hz, 1H), 6.90 (d, J = 8.0 Hz, 2H), 4.81 (td, J = 9.6, 4.7 Hz, 1H), 3.44–3.31 (m, 2H), 2.14 (s, 3H). ^{13}C NMR (101 MHz, DMSO-d_6) δ 148.8, 141.7, 141.7, 139.3, 138.3, 136.5 (2C), 135.4, 131.3 (2C), 130.5 (2C), 130.4, 129.8, 128.5 (2C), 128.5 (2C), 127.0, 126.7, 125.5 (2C), 123.6, 122.7, 120.4, 55.1, 37.7, 20.9. LC/MS ESI + t_R 7.683. HRMS (+ESI): 692.9618 $[M+H]^+$. Calculated for $C_{28}H_{22}BrCl_2N_4O_4S_2$: 692.9615.

4.1.5.5. N-(2-{6-chloro-8-[(4-chlorophenyl)thio]-3-nitroimidazo[1,2-a] pyridin-2-yl}-1-(4-cyanophenyl)ethyl)-4-methylbenzenesulfonamide (6e). Starting from NaH 60 % (28 mg, 0.70 mmol), 4-chlorothiophenol (101 mg, 0.70 mmol) and *N*-[2-(8-Bromo-6-chloro-3-nitroimidazo[1,2-*a*] pyridin-2-yl)-1-(4-cyanophenyl)ethyl]-4-methylbenzenesulfonamide **(4k)** (0.35 mmol), the mixture was slowly poured into 100 mL of an ice-water mixture and precipitated. The solid was collected by filtration and dried under reduced pressure. Compound **(6d)** was obtained after purification by chromatography on silica gel (eluent: cyclohexane-dichloromethane-ethyl acetate gradient from 5:5:0 to 0:9:1) as a yellow solid in 74 % yield (165 mg, 0.26 mmol).

mp 235 °C. ^{1}H NMR (400 MHz, DMSO-d_6) δ 9.03 (d, J = 1.8 Hz, 1H), 8.82 (d, J = 9.4 Hz, 1H), 7.84–7.78 (m, 2H), 7.77–7.69 (m, 2H), 7.69–7.64 (m, 2H), 7.62–7.57 (m, 2H), 7.27–7.19 (m, 2H), 6.99 (d, J = 1.9 Hz, 1H), 6.91 (d, J = 8.1 Hz, 2H), 4.93–4.81 (m, 1H), 3.47–3.34 (m, 2H), 2.14 (s, 3H). ^{13}C NMR (101 MHz, DMSO-d_6) δ 148.5, 147.6, 141.8, 139.3, 138.1, 136.5 (2C), 135.4, 132.5 (2C), 130.6 (2C), 130.4, 129.9, 128.6 (2C), 127.4 (2C), 126.9, 126.8, 125.5 (2C), 123.6, 122.7, 118.7, 110.1, 55.4, 37.4, 20.9. LC/MS ESI + t_R 7.297, *(m/z)* $[M+H]^+$ 638.13/639.19/640.19. HRMS (+ESI): 638.0482 $[M+H]^+$. Calculated for $C_{29}H_{22}Cl_2N_5O_4S_2$: 638.0485.

4.1.6. Preparation of N-(2-{6-chloro-8-[(4-chlorophenyl)sulfinyl]-3-nitroimidazo[1,2-a]pyridin-2-yl}-1-(4-chlorophenyl)ethyl)-4-methylbenzenesulfonamide (7)

To a solution of *N*-(2-{6-Chloro-8-[(4-chlorophenyl)thio]-3-nitroimidazo[1,2-*a*]pyridin-2-yl}-1-(4-chlorophenyl)ethyl)-4-methylbenzenesulfonamide **(6b)** (200 mg, 0.31 mmol, 1 equiv) in dichloromethane (20 mL) at 0 °C, *meta*-chloroperoxybenzoic acid (52 mg, 0.31 mmol, 1 equiv) was added. The reaction mixture was stirred for 3 h at 0 °C and then slowly poured into 100 mL of an ice-water mixture. The mixture was extracted three times with 70 mL of dichloromethane, then the organic layer was dried over anhydrous Na_2SO_4, filtered, and evaporated. Compound **(7)** was obtained after purification by chromatography on silica gel (eluent: dichloromethane-ethyl acetate gradient from 100:0 to 85:15) as a pale yellow solid in 63 % yield (130 mg, 0.20 mmol).

mp 196 °C. ^{1}H NMR (400 MHz, DMSO-d_6) δ 9.24 (d, J = 1.9 Hz, 1H), 8.60 (d, J = 9.3 Hz, 1H), 8.16 (d, J = 2.0 Hz, 1H), 7.99–7.94 (m, 2H), 7.64–7.59 (m, 2H), 7.42–7.35 (m, 4H), 7.16–7.10 (m, 2H), 6.85 (d, J = 8.0 Hz, 2H), 4.91–4.82 (m, 1H), 3.47–3.35 (m, 2H), 2.19 (s, 3H). ^{13}C NMR (101 MHz, DMSO-d_6) 149.3, 141.8, 141.7, 140.9, 137.3, 136.9, 134.9, 133.3, 131.9, 130.7, 129.7 (2C), 128.6 (2C), 128.3 (4C), 127.6, 127.1 (2C), 126.2, 125.5 (2C), 123.6, 55.4, 37.5, 20.9. LC/MS ESI + t_R 7.340, *(m/z)* $[M+H]^+$ 663.10/665.03. HRMS (+ESI): 665.0066 $[M+H]^+$. Calculated for $C_{28}H_{22}Cl_3N_4O_5S_2$: 665.0066.

4.1.7. Preparation of N-(2-{6-chloro-8-[(4-chlorophenyl)sulfonyl]-3-nitroimidazo[1,2-a]pyridin-2-yl}-1-(4-chlorophenyl)ethyl)-4-methylbenzenesulfonamide (8)

To a solution of *N*-(2-{6-Chloro-8-[(4-chlorophenyl)thio]-3-nitroimidazo[1,2-*a*]pyridin-2-yl}-1-(4-chlorophenyl)ethyl)-4-methylbenzenesulfonamide **(6b)** (200 mg, 0.31 mmol, 1 equiv) in dichloromethane (20 mL), *meta*-chloroperoxybenzoic acid (104 mg, 0.62 mmol, 2 equiv) was added. The reaction mixture was stirred for 24 h at room temperature and then slowly poured into 100 mL of an ice-water mixture. The mixture was extracted three times with 70 mL of dichloromethane, then the organic layer was dried over anhydrous Na_2SO_4, filtered, and evaporated. Compound **(8)** was obtained after purification by chromatography on silica gel (eluent: dichloromethane-ethyl acetate gradient from 100:0 to 95:5) as a white solid in 21 % yield (44 mg, 0.065 mmol).

mp 247 °C. ^{1}H NMR (400 MHz, DMSO-d_6) δ 9.36 (d, J = 2.0 Hz, 1H), 8.52 (d, J = 2.0 Hz, 1H), 8.42–8.32 (m, 3H), 7.86–7.76 (m, 2H), 7.37 (s, 4H), 6.80 (d, J = 8.0 Hz, 2H), 6.71 (d, J = 8.0 Hz, 2H), 4.79–4.66 (m, 1H), 3.51–3.35 (m, 2H), 2.16 (s, 3H). ^{13}C NMR (101 MHz, DMSO-d_6) δ 149.3, 142.0, 140.8, 140.4, 137.9, 137.2, 137.2, 132.9, 132.0, 131.5 (2C), 130.7, 130.4, 129.8 (2C), 128.4 (2C), 128.3 (2C), 128.3 (2C), 128.3, 125.5 (2C), 122.4, 54.9, 37.4, 20.9. LC/MS ESI + t_R 7.247, *(m/z)* $[M+H]^+$ 679.27/681.28. HRMS (+ESI): 681.0016 $[M+H]^+$. Calculated for $C_{28}H_{22}Cl_3N_4O_6S_2$: 681.0016.

4.1.8. General procedure for the preparation of N-{2-[6-chloro-3-nitro-8-(pyridin-4-yl)imidazo[1,2-a]pyridin-2-yl]-1-phenylethyl}-4-methylbenzenesulfonamide derivatives (9a–e)

To a solution of the appropriate *N*-[2-(8-Bromo-6-chloro-3-nitro-imidazo[1,2-*a*]pyridin-2-yl)-1-phenylethyl]-4-methyl-benzenesulfonamide (200 mg, 1 equiv) and K_2CO_3 (5 equiv) in tetrahydrofuran (10 mL) at room temperature were added 4-pyridinyl-boronic acid (1.5 equiv) and Pd(dppf)Cl_2 (0.1 equiv). The reaction mixture was sealed and placed under an inert atmosphere. The reaction mixture was then heated for the appropriate duration at 120 °C under microwave irradiation.

4.1.8.1. N-{2-[6-chloro-3-nitro-8-(pyridin-4-yl)imidazo[1,2-a]pyridin-2-yl]-1-(4-fluorophenyl)ethyl}-4-methylbenzenesulfonamide (9a). Starting from *N*-[2-(8-Bromo-6-chloro-3-nitroimidazo[1,2-*a*]pyridin-2-yl)-1-(4-fluorophenyl)ethyl]-4-methylbenzenesulfonamide **(4e)** (0.35 mmol), K_2CO_3 (243 mg, 1.76 mmol), 4-pyridinylboronic acid (65 mg, 0.53 mmol) and Pd(dppf)Cl_2 (26 mg, 0.035 mmol) heated 2 h, the mixture was slowly poured into 100 mL of an ice-water mixture and precipitated. The solid was collected by filtration and dried under reduced pressure. Compound **(9a)** was obtained after purification by chromatography on silica gel (eluent: dichloromethane-ethyl acetate gradient from 10:0 to 6:4) as a yellow solid in 40 % yield (79 mg, 0.14 mmol).

mp 277 °C. ^{1}H NMR (400 MHz, DMSO-d_6) δ 9.30 (d, J = 2.0 Hz, 1H), 8.79 (d, J = 4.9 Hz, 2H), 8.62 (d, J = 9.2 Hz, 1H), 8.29 (d, J = 2.0 Hz, 1H), 8.07–7.94 (m, 2H), 7.48–7.41 (m, 2H), 7.25–7.20 (m, 2H), 7.20–7.13 (m, 2H), 6.88 (d, J = 8.0 Hz, 2H), 4.94–4.84 (m, 1H), 3.40 (s, 1H), 3.39 (d, J = 4.2 Hz, 1H), 2.17 (s, 3H). ^{13}C NMR (101 MHz, DMSO-d_6) δ 161.3 (d, J = 243.0 Hz), 150.0 (2C), 149.5, 141.7, 140.6, 140.5, 138.6 (d, J = 3.3 Hz), 138.5, 130.9, 130.3, 128.8, 128.5 (2C), 128.3 (d, J = 8.1 Hz, 2C), 126.9, 125.8, 125.4 (2C), 123.8, 123.8, 115.08 (d, J = 21.5 Hz, 2C), 55.0, 38.0, 20.9. LC/MS ESI + t_R 6.813, *(m/z)* $[M+H]^+$ 566.02. HRMS (+ESI): 566.1061 $[M+H]^+$. Calculated for $C_{27}H_{22}ClFN_5O_4S$: 566.1060.

4.1.8.2. N-{2-[6-chloro-3-nitro-8-(pyridin-4-yl)imidazo[1,2-a]pyridin-2-yl]-1-(4-chlorophenyl)ethyl}-4-methylbenzenesulfonamide (9b). Starting from *N*-[2-(8-Bromo-6-chloro-3-nitroimidazo[1,2-*a*]pyridin-2-yl)-1-(4-chlorophenyl)ethyl]-4-methylbenzenesulfonamide **(4g)** (0.34 mmol), K_2CO_3 (236 mg, 1.71 mmol), 4-pyridinylboronic acid (63 mg, 0.51 mmol) and Pd(dppf)Cl_2 (25 mg, 0.034 mmol) heated 1 h, the mixture was slowly poured into an 100 mL of ice-water mixture. The mixture was extracted three times with 70 mL of dichloromethane, then the organic layer was dried over anhydrous Na_2SO_4, filtered, and evaporated. Compound **(9b)** was obtained after purification by chromatography on silica gel (eluent: dichloromethane-ethyl acetate gradient from 10:0 to 6:4) as a yellow solid in 44 % yield (87 mg, 0.15 mmol).

mp 250 °C. ^{1}H NMR (400 MHz, DMSO-d_6) δ 9.31 (d, J = 1.9 Hz, 1H), 8.78 (s, 2H), 8.64 (d, J = 9.2 Hz, 1H), 8.29 (d, J = 2.0 Hz, 1H), 7.99 (d, J = 5.6 Hz, 2H), 7.44–7.37 (m, 4H), 7.23 (d, J = 8.0 Hz, 2H), 6.89 (d, J = 7.9 Hz, 2H), 4.95–4.75 (m, 1H), 3.41 (s, 1H), 3.39 (d, J = 3.3 Hz, 1H), 2.18 (s, 3H). ^{13}C NMR (101 MHz, DMSO-d_6) δ 150.0 (2C), 149.4, 141.8, 141.3, 140.5, 140.5, 138.5, 131.8, 130.9, 130.3, 128.6 (2C), 128.4, 128.3 (2C), 128.3 (2C), 126.9, 125.8, 125.4 (2C), 123.8 (2C), 55.1, 37.7, 20.9. LC/MS ESI + t_R 7.017, *(m/z)* $[M+H]^+$ 582.02/584.02. HRMS (+ESI): 582.0768 $[M+H]^+$. Calculated for $C_{27}H_{22}Cl_2N_5O_4S$: 582.0764.

4.1.8.3. N-{2-[6-chloro-3-nitro-8-(pyridin-4-yl)imidazo[1,2-a]pyridin-2-yl]-1-(3-chlorophenyl)ethyl}-4-methylbenzenesulfonamide (9c). Starting from *N*-[2-(8-Bromo-6-chloro-3-nitroimidazo[1,2-*a*]pyridin-2-yl)-1-(3-chlorophenyl)ethyl]-4-methylbenzenesulfonamide **(4h)** (0.34 mmol), K_2CO_3 (236 mg, 1.71 mmol), 4-pyridinylboronic acid (63 mg, 0.51 mmol) and Pd(dppf)Cl_2 (25 mg, 0.034 mmol) heated 1 h, the mixture was slowly poured into 100 mL of an ice-water mixture. The mixture was extracted three times with 70 mL of dichloromethane, then the organic layer was dried over anhydrous Na_2SO_4, filtered, and evaporated. Compound **(9c)** was obtained after purification by chromatography on silica gel (eluent: dichloromethane-ethyl acetate gradient from 10:0 to 6:4) as a pale yellow solid in 60 % yield (119 mg, 0.20 mmol).

mp 271 °C. ^{1}H NMR (400 MHz, DMSO-d_6) δ 9.32 (d, J = 1.9 Hz, 1H), 8.79 (s, 2H), 8.65 (d, J = 9.3 Hz, 1H), 8.30 (d, J = 2.0 Hz, 1H), 8.01 (d, J = 5.5 Hz, 2H), 7.44 (s, 1H), 7.38–7.29 (m, 3H), 7.24 (d, J = 8.2 Hz, 2H), 6.89 (d, J = 7.9 Hz, 2H), 4.93–4.83 (m, 1H), 3.47–3.36 (m, 2H), 2.18 (s, 3H). ^{13}C NMR (101 MHz, DMSO-d_6) δ 150.0 (2C), 149.3, 144.6, 141.9, 140.5, 140.5, 138.3, 133.1, 131.0, 130.3, 130.3, 128.8, 128.6 (2C), 127.2, 126.9, 126.3, 125.8, 125.4 (2C), 125.2, 123.8, 123.8, 55.2, 37.7, 20.9. LC/MS ESI + t_R 6.947, *(m/z)* $[M+H]^+$ 582.23/583.09/584.21/585.07. HRMS (+ESI): 582.0763 $[M+H]^+$. Calculated for $C_{27}H_{22}Cl_2N_5O_4S$: 582.0764.

4.1.8.4. N-{2-[6-chloro-3-nitro-8-(pyridin-4-yl)imidazo[1,2-a]pyridin-2-yl]-1-(4-bromophenyl)ethyl}-4-methylbenzenesulfonamide (9d). Starting from *N*-[2-(8-Bromo-6-chloro-3-nitroimidazo[1,2-*a*]pyridin-2-yl)-1-(4-bromophenyl)ethyl]-4-methylbenzenesulfonamide **(4j)** (0.32 mmol), K_2CO_3 (220 mg, 1.59 mmol), 4-pyridinylboronic acid (59 mg, 0.48 mmol) and Pd(dppf)Cl_2 (23 mg, 0.032 mmol) heated 2 h, the mixture was slowly poured into 100 mL of an ice-water mixture. The mixture was extracted three times with 70 mL of dichloromethane, then the organic layer was dried over anhydrous Na_2SO_4, filtered, and evaporated. Compound **(9d)** was obtained after purification by chromatography on silica gel (eluent: dichloromethane-ethyl acetate gradient from 10:0 to 6:4) as a yellow solid in 36 % yield (72 mg, 0.12 mmol).

mp 260 °C. ^{1}H NMR (400 MHz, DMSO-d_6) δ 9.31 (d, J = 1.9 Hz, 1H), 8.83–8.73 (m, 2H), 8.64 (d, J = 9.2 Hz, 1H), 8.29 (d, J = 2.0 Hz, 1H), 8.02–7.93 (m, 2H), 7.56–7.48 (m, 2H), 7.38–7.33 (m, 2H), 7.26–7.18 (m, 2H), 6.89 (d, J = 8.0 Hz, 2H), 4.90–4.79 (m, 1H), 3.41 (s, 1H), 3.39 (d, J = 2.0 Hz, 1H), 2.18 (s, 3H). ^{13}C NMR (101 MHz, DMSO-d_6) δ 150.0 (2C), 149.3, 141.8, 141.6, 140.5, 140.5, 138.4, 131.2 (2C), 130.9, 130.3, 128.8, 128.7 (2C), 128.6 (2C), 126.9, 125.8, 125.5 (2C), 123.8, 123.7, 120.4, 55.1, 37.6, 20.9. LC/MS ESI + t_R 7.070, *(m/z)* $[M+H]^+$ 625.96/628.04. HRMS (+ESI): 628.0239 $[M+H]^+$. Calculated for $C_{27}H_{22}BrClN_5O_4S$: 628.0239.

4.1.8.5. N-{2-[6-chloro-3-nitro-8-(pyridin-4-yl)imidazo[1,2-a]pyridin-2-yl]-1-(4-cyanophenyl)ethyl}-4-methylbenzenesulfonamide (9e). Starting from *N*-[2-(8-Bromo-6-chloro-3-nitroimidazo[1,2-*a*]pyridin-2-yl)-1-(4-cyanophenyl)ethyl]-4-methylbenzenesulfonamide **(4k)** (0.35 mmol), K_2CO_3 (240 mg, 1.74 mmol), 4-pyridinylboronic acid (64 mg, 0.52 mmol) and Pd(dppf)Cl_2 (26 mg, 0.035 mmol) heated 1 h, the mixture was slowly poured into 100 mL of an ice-water mixture and precipitated. The solid was collected by filtration and dried under reduced pressure. Compound **(9e)** was obtained after purification by chromatography on silica gel (eluent: dichloromethane-ethyl acetate gradient from 10:0 to 5:5) as a yellow solid in 25 % yield (50 mg, 0.088 mmol).

mp 263 °C. ^{1}H NMR (400 MHz, DMSO-d_6) δ 9.31 (d, J = 1.9 Hz, 1H), 8.81–8.72 (m, 3H), 8.29 (d, J = 2.0 Hz, 1H), 8.00–7.94 (m, 2H), 7.84–7.77 (m, 2H), 7.63–7.56 (m, 2H), 7.27–7.21 (m, 2H), 6.89 (d, J = 8.1 Hz, 2H), 4.99–4.88 (m, 1H), 3.43 (d, J = 2.2 Hz, 1H), 3.41 (d, J = 5.4 Hz, 1H), 2.18 (s, 3H). ^{13}C NMR (101 MHz, DMSO-d_6) δ 150.0 (2C), 149.0, 147.6, 142.0, 140.5, 140.5, 138.2, 132.5, 132.4 (2C), 131.0, 130.3, 128.6 (2C), 127.5 (2C), 126.9, 125.8, 125.5 (2C), 123.9, 123.7, 118.7, 110.1, 55.4, 37.4, 20.9. LC/MS ESI + t_R 6.567, *(m/z)* $[M+H]^+$ 573.03/575.04. HRMS (+ESI): 573.1105 $[M+H]^+$. Calculated for $C_{28}H_{22}ClN_6O_4S$: 573.1106.

4.2. Electrochemistry

Voltammetric measurements were carried out with a potentiostat Autolab PGSTAT100 (ECO Chemie, The Netherlands) controlled by GPES 4.09 software. Experiments were performed at room temperature

in a homemade airtight three electrode cell connected to a vacuum/argon line. The reference electrode consisted of a saturated calomel electrode (SCE) separated from the solution by a bridge compartment. The counter electrode was a platinum wire of 1 cm^2 apparent surface. The working electrode was GC microdisk (1.0 mm of diameter e Biologic SAS). The supporting electrolyte (nBu_4N)[PF_6] (Fluka, 99 % puriss electrochemical grade) and the solvent DMSO (Sigma-Aldrich puriss p.a. dried <0.02 % water) were used as received and simply degassed under argon. The solutions used during the electrochemical studies were typically 10^{-3} M in compound and 0.1 M in supporting electrolyte.

Before each measurement, the solutions were degassed by bubbling Ar and the working electrode was polished with a polishing machine (Presi P230, Eybens, France). Under these experimental conditions employed in this work, the half-wave potential ($E_{1/2}$) of the ferrocene Fc^+/Fc couple in DMSO was $E_{1/2} = 0.46$ V vs SCE. Experimental peak potentials have been measured versus SCE and converted to SHE by adding 0.241 V.

4.3. Biology

4.3.1. Antileishmanial activity on L. infantum axenic amastigotes

L. infantum promastigotes (MHOM/MA/67/ITMAP-263, CNR Leishmania, Montpellier, France, expressing luciferase activity) were used in the following tests. *L. infantum* promastigotes were harvested in logarithmic phase of growth by centrifugation at 900*g* for 10 min. The supernatant was removed carefully and was replaced by the same volume of RPMI 1640 complete medium at pH 5.4 and incubated for 24 h at 24 °C. The acidified promastigotes were then incubated for 24 h at 37 °C in a ventilated flask to transform them into axenic amastigotes. The amastigote stage was confirmed by both electron microscopy (characterized by a short flagellum with a small, bulbous tip extending beyond a spherical cell body) and RT-PCR, which demonstrated the overexpression of ATG8 and amastin genes in amastigotes, compared to promastigotes. The effects of the tested compounds on the growth of *L. infantum* axenic amastigotes were assessed as follows. *L. infantum* amastigotes were incubated at a density of 2×10^6 parasites/mL in sterile 96-well plates with various concentrations of compounds dissolved in DMSO (final concentration less than 0.5 % *v/v*), in duplicate. Appropriate controls treated with DMSO, amphotericin B, and miltefosine were added to each set of experiments. After a 48 h incubation period at 37 °C, each plate-well was then microscopically examined to detect any precipitate formation. To estimate the luciferase activities of promastigotes, 80 µl of each well are transferred to white 96-well plates, Steady Glow reagent (Promega) was added according to the manufacturer's instructions, and plates were incubated for 2 min. The luminescence was measured in a FLUOstar Omega (BMG Labtech). Efficient concentration 50 % (IC_{50}) was defined as the concentration of drug required to inhibit by 50 % the metabolic activity of *L. infantum* axenic amastigotes compared to the control. IC_{50} were calculated by nonlinear regression analysis processed on dose–response curves, using TableCurve 2D V5 software.

4.3.2. Antileishmanial activity on L. infantum intracellular amastigotes

The undifferentiated THP1 human monocyte cells (acute monocytic leukemia cell line purchased from ATCC, ref TIB-202) were grown in RPMI 1640 medium (Life Technologies, Saint-Aubin, France) supplemented with 10 % FCS (Life Technologies, Saint-Aubin, France), 100 U/mL penicillin, 100 µg/mL streptomycin and 2 mM L-glutamine at 37 °C, 5 % CO2. The culture was maintained between 3.10^5 and 1.10^6 cells/mL. The *in vitro* evaluation of the antileishmanial activity on intracellular amastigote forms of the tested compound was assessed as below. Briefly, 200 µL of THP-1 cells with Phorbol 12-Myristate 13-Acetate (final concentration 50 ng/mL) were seeded in 96-well plates at an average density of 0.77×10^5 cells/mL and incubated for 96 h at 37 °C, 5 % CO_2. Promastigotes were centrifuged at 3000 rpm, for 10 min and the supernatant was replaced with the same volume of complete RPMI pH 5.4 and incubated for 24 h at 27 °C. Differentiated THP-1 cells were then infected with acidified promastigotes at an infection ratio of 20 parasites per macrophage and incubated for 24 h at 37 °C, 5 % CO_2. Plates were rinsed three times, and then, in duplicate, medium containing various concentrations of reference drugs and DMSO was added (final DMSO concentrations below 0.5 % *v/v*). The plates were then incubated for 120 h. *Luciferase activity and determination of IC_{50} were performed as above.*

4.3.3. Cytotoxicity on THP1 cell line

200 µL of THP1 cells with Phorbol 12-Myristate 13-Acetate (final concentration 50 ng/mL) were seeded in 96-well plates at an average density of 0.77×10^5 cells/mL and incubated for 96 h at 37 °C, 5 % CO_2. Various concentrations of compounds dissolved in DMSO (final concentration less than 0.5 % v/v), and references in duplicate were then added. The plates were incubated for 72 h at 37 °C. Each well plate was then microscope-examined for detecting possible precipitate formation before the medium was aspirated from the wells. 100 µL of MTT solution (0.5 mg/mL in medium) were then added to each well. Cells were incubated for 2 h at 37 °C. After this time, the MTT solution was removed and DMSO (100 µL) was added to dissolve the resulting blue formazan crystals. The plates were shaken vigorously (300 rpm) for 10 min. The absorbance was measured at 570 nm using a BIO-TEK ELx808 Absorbance Microplate Reader. DMSO was used as blank and doxorubicin (purchased from Sigma Aldrich) as positive control. Cell viability was calculated as percentage of control (cells incubated with DMSO). The 50 % cytotoxic concentration (CC_{50}) was determined from the dose–response curve by using the TableCurve 2D V5 software. CC_{50} values represent the mean value calculated from three separate experiments.

4.3.4. Thermodynamic solubility at pH 7.4

Thermodynamic solubility at pH 7.4 of compounds was determined according to a miniaturized shake-flask method (Organisation for Economic Cooperation and Development guideline n°105) [26]. Phosphate Buffer solutions (pH 7.4, 10 µM, ionic strength 150 µM) were prepared from Na_2HPO_4, KH_2PO_4 and KCl (Sigma Aldrich, Saint Quentin Fallavier, France); 10 µL of 20 mM stock solution were added to 5 mL glass tubes containing 990 mL buffer ($n = 3$). The tubes were briefly sonicated and shacked by inversion during 24 h at 23 °C. Then, the tube contents were placed in a microtube which was centrifuged at 12,225×*g* for 10 min; 100 µL supernatant were mixed with 100 µL acetonitrile in a Greiner UV microplate. Standard solutions were prepared extemporaneously, diluting 20 mM DMSO stock solutions at 0, 5, 10 and 20 mM; 5 µL of each working solution were diluted with 995 µL buffer and 100 µL were then mixed in microplates with 100 µL acetonitrile so as to ensure that the final proportions of each solvent in standard solutions and samples remained unchanged. Solubility at pH 7.4 was determined with an Infinite M200Pro (Tecan, Lyon, France) microplate reader in spectrophotometric mode (230–450 nm) from the specific λ_{max} of each compound. The calibration curve was obtained from the three standard solutions of tested compounds at 0, 25, 50, and 100 µM in a 50:50 (vol/vol) mixture of buffer with acetonitrinile/DMSO (99:1; vol/vol). Calibration curves were linear with $R^2 > 0.99$.

CRediT authorship contribution statement

Inès Jacquet: Writing – original draft, Investigation, Formal analysis. **Romain Paoli-Lombardo:** Writing – review & editing. **Caroline Castera-Ducros:** Writing – review & editing. **Hugo Pomares:** Writing – review & editing, Investigation. **Sandra Bourgeade-Delmas:** Writing – review & editing, Investigation, Formal analysis. **Patrice Vanelle:** Writing – review & editing, Supervision, Resources, Project administration. **Nicolas Primas:** Writing – review & editing, Validation, Supervision, Project administration, Methodology, Conceptualization.

Funding

This research did not receive any specific grant from funding agencies in the public, commercial, or not-for-profit sectors.

Declaration of competing interest

The authors declare that they have no known competing financial interests or personal relationships that could have appeared to influence the work reported in this paper.

Acknowledgements

We want to thank Vincent Remusat (Institut de Chimie Radicalaire, Marseille) for his help with NMR analysis, Valérie Monnier and Gaëlle Hisler (Spectropole, Marseille) for performing HRMS analysis, Dimitri Fayolle and Marc Since (Platform DruiD, Centre d'Etudes et de Recherche sur le Médicament de Normandie, Caen) for performing solubility measurement and Alix Sournia-Saquet (Laboratoire de chimie de coordination, Toulouse) for performing electrochemistry analysis.

Appendix A. Supplementary data

Supplementary data to this article can be found online at https://doi.org/10.1016/j.ejmech.2025.118506.

Data availability

Data will be made available on request.

References

[1] Neglected tropical diseases , (n.d.). https://www.who.int/news-room/questions-and-answers/item/neglected-tropical-diseases (accessed July 17, 2025).
[2] S. Burza, S.L. Croft, M. Boelaert, Leishmaniasis, Lancet 392 (2018) 951–970, https://doi.org/10.1016/S0140-6736(18)31204-2.
[3] Leishmaniasis , (n.d.). https://www.who.int/news-room/fact-sheets/detail/leishmaniasis (accessed July 17, 2025).
[4] S. Pradhan, R.A. Schwartz, A. Patil, S. Grabbe, M. Goldust, Treatment options for leishmaniasis, Clin. Exp. Dermatol. 47 (2022) 516–521, https://doi.org/10.1111/ced.14919.
[5] Research & development portfolio, DNDi. https://dndi.org/wp-content/uploads/2025/01/DNDi-RD-Portfolio-December-2024.pdf, 2024 (accessed July 4, 2025).
[6] A.M. Rice, Y. Long, S.B. King, Nitroaromatic antibiotics as nitrogen oxide sources, Biomolecules 11 (2021) 267, https://doi.org/10.3390/biom11020267.
[7] S.T. Abreu, L.G.V. Gelves, E.J. Barreiro, L.M. Lima, Revisiting nitroaromatic drugs: mechanisms of bioactivation, metabolism and toxicity and methods to synthesize nitroaromatic fragments, J. Braz. Chem. Soc. 35 (2024) e, https://doi.org/10.21577/0103-5053.20240071.
[8] ICH guideline S2 (R1), On Genotoxicity Testing and Data Interpretation for Pharmaceuticals Intended for Human Use, European Medicine Agency, 2012. https://www.ema.europa.eu/en/documents/scientific-guideline/ich-guideline-s2-r1-genotoxicity-testing-and-data-interpretation-pharmaceuticals-intended-human-use-step-5_en.pdf. (Accessed 10 July 2025).
[9] A.K. Lindner, V. Lejon, F. Chappuis, J. Seixas, L. Kazumba, M.P. Barrett, E. Mwamba, O. Erphas, E.A. Akl, G. Villanueva, H. Bergman, P. Simarro, A. Kadima Ebeja, G. Priotto, J.R. Franco, New WHO guidelines for treatment of gambiense human African trypanosomiasis including fexinidazole: substantial changes for clinical practice, Lancet Infect. Dis. 20 (2020) e38–e46, https://doi.org/10.1016/S1473-3099(19)30612-7.
[10] A.K. Lindner, V. Lejon, M.P. Barrett, L. Blumberg, S.A. Bukachi, R.J. Chancey, A. Edielu, L. Matemba, T. Mesha, V. Mwanakasale, C. Pasi, T. Phiri, J. Seixas, E. A. Akl, K. Probyn, G. Villanueva, P.P. Simarro, A.K. Ebeja, J.R. Franco, G. Priotto, New WHO guidelines for treating rhodesiense human African trypanosomiasis: expanded indications for fexinidazole and pentamidine, Lancet Infect. Dis. 25 (2025) e77–e85, https://doi.org/10.1016/S1473-3099(24)00581-4.
[11] V. Dällenbach, DNDI-0690, DNDi. https://dndi.org/research-development/portfolio/dndi-0690/, 2014. (Accessed 7 July 2025).
[12] C. Castera-Ducros, L. Paloque, P. Verhaeghe, M. Casanova, C. Cantelli, S. Hutter, F. Tanguy, M. Laget, V. Remusat, A. Cohen, M.D. Crozet, P. Rathelot, N. Azas, P. Vanelle, Targeting the human parasite *Leishmania donovani*: discovery of a new promising anti-infectious pharmacophore in 3-nitroimidazo[1,2-a]pyridine series, Bioorg. Med. Chem. 21 (2013) 7155–7164, https://doi.org/10.1016/j.bmc.2013.09.002.
[13] C. Fersing, C. Boudot, R. Paoli-Lombardo, N. Primas, E. Pinault, S. Hutter, C. Castera-Ducros, Y. Kabri, J. Pedron, S. Bourgeade-Delmas, A. Sournia-Saquet, J.-L. Stigliani, A. Valentin, A. Azqueta, D. Muruzabal, A. Destere, S. Wyllie, A. H. Fairlamb, S. Corvaisier, M. Since, A. Malzert-Fréon, C. Di Giorgio, P. Rathelot, N. Azas, B. Courtioux, P. Vanelle, P. Verhaeghe, Antikinetoplastid SAR study in 3-nitroimidazopyridine series: identification of a novel non-genotoxic and potent anti-*T. b. brucei* hit-compound with improved pharmacokinetic properties, Eur. J. Med. Chem. 206 (2020) 112668, https://doi.org/10.1016/j.ejmech.2020.112668.
[14] C. Fersing, L. Basmaciyan, C. Boudot, J. Pedron, S. Hutter, A. Cohen, C. Castera-Ducros, N. Primas, M. Laget, M. Casanova, S. Bourgeade-Delmas, M. Piednoel, A. Sournia-Saquet, V. Belle Mbou, B. Courtioux, É. Boutet-Robinet, M. Since, R. Milne, S. Wyllie, A.H. Fairlamb, A. Valentin, P. Rathelot, P. Verhaeghe, P. Vanelle, N. Azas, Nongenotoxic 3-Nitroimidazo[1,2-a]pyridines are NTR1 substrates that display potent in vitro antileishmanial activity, ACS Med. Chem. Lett. 10 (2019) 34–39, https://doi.org/10.1021/acsmedchemlett.8b00347.
[15] R. Paoli-Lombardo, N. Primas, S. Bourgeade-Delmas, S. Hutter, A. Sournia-Saquet, C. Boudot, E. Brenot, C. Castera-Ducros, S. Corvaisier, M. Since, A. Malzert-Fréon, B. Courtioux, A. Valentin, P. Verhaeghe, N. Azas, P. Rathelot, P. Vanelle, Improving aqueous solubility and in vitro pharmacokinetic properties of the 3-Nitroimidazo [1,2-a]pyridine antileishmanial pharmacophore, Pharmaceuticals 15 (2022) 998, https://doi.org/10.3390/ph15080998.
[16] G. Giuglio-Tonolo, T. Terme, M. Médebielle, P. Vanelle, Original reaction of p-nitrobenzyl chloride with aldehydes using tetrakis(dimethylamino)ethylene (TDAE), Tetrahedron Lett. 44 (2003) 6433–6435, https://doi.org/10.1016/S0040-4039(03)01594-6.
[17] M. Montana, M.D. Crozet, C. Castera-Ducros, T. Terme, P. Vanelle, Rapid synthesis of new azaheterocyclic hydroxymalonate derivatives using TDAE approach, Heterocycles 75 (2008) 925, https://doi.org/10.3987/com-07-11264.
[18] T. Juspin, M. Laget, T. Terme, N. Azas, P. Vanelle, TDAE-assisted synthesis of new imidazo[2,1- b]thiazole derivatives as anti-infectious agents, Eur. J. Med. Chem. 45 (2010) 840–845, https://doi.org/10.1016/j.ejmech.2009.10.048.
[19] M. Roche, T. Terme, P. Vanelle, Original TDAE strategy using propargylic chloride: rapid access to 1,4-Diarylbut-3-ynol derivatives, Molecules 18 (2013) 1540–1548, https://doi.org/10.3390/molecules18021540.
[20] H. Sharghi, M. Hosseini-Sarvari, S. Ebrahimpourmoghaddam, A novel method for the synthesis of N-sulfonyl aldimines using AlCl3 under solvent-free conditions (SFC), ARKIVOC (Gainesville, FL, U. S.) 2007 (2007) 255–264, https://doi.org/10.3998/ark.5550190.0008.f25.
[21] C. Fersing, C. Boudot, C. Castera-Ducros, E. Pinault, S. Hutter, R. Paoli-Lombardo, N. Primas, J. Pedron, L. Seguy, S. Bourgeade-Delmas, A. Sournia-Saquet, J.-L. Stigliani, J.-Y. Brossas, L. Paris, A. Valentin, S. Wyllie, A.H. Fairlamb, É. Boutet-Robinet, S. Corvaisier, M. Since, A. Malzert-Fréon, A. Destere, D. Mazier, P. Rathelot, B. Courtioux, N. Azas, P. Verhaeghe, P. Vanelle, 8-Alkynyl-3-nitroimidazopyridines display potent antitrypanosomal activity against both *T. b. brucei* and *cruzi*, Eur. J. Med. Chem. 202 (2020) 112558, https://doi.org/10.1016/j.ejmech.2020.112558.
[22] C. Fersing, Synthèse et étude des relations structure-activité de nouvelles 3-nitro-imidazo (1,2-a) pyridines Anti-kinétoplastidés, These de doctorat, Aix-Marseille, 2018. https://theses.fr/2018AIXM0275. (Accessed 28 July 2025).
[23] R. Paoli-Lombardo, Synthèse et étude de l'activité Anti-kinétoplastidés de nouveaux dérivés nitroaromatiques, Thèse de doctorat, Aix-Marseille Université, 2022. https://theses.fr/2022AIXM0600.
[24] C. Fersing, Synthèse et étude des relations structure-activité de nouvelles 3-nitroimidazo[1,2-*a*]pyridines Anti-kinétoplastidés, Thèse de doctorat, Aix-Marseille Université, 2018. https://theses.fr/2018AIXM0275.
[25] W. McCoull, S. Boyd, M.R. Brown, M. Coen, O. Collingwood, N.L. Davies, A. Doherty, G. Fairley, K. Goldberg, E. Hardaker, G. He, E.J. Hennessy, P. Hopcroft, G. Hodgson, A. Jackson, X. Jiang, A. Karmokar, A.-L. Lainé, N. Lindsay, Y. Mao, R. Markandu, L. McMurray, N. McLean, L. Mooney, H. Musgrove, J.W.M. Nissink, A. Pflug, V.P. Reddy, P.B. Rawlins, E. Rivers, M. Schimpl, G.F. Smith, S. Tentarelli, J. Travers, R.I. Troup, J. Walton, C. Wang, S. Wilkinson, B. Williamson, J. Winter-Holt, D. Yang, Y. Zheng, Q. Zhu, P.D. Smith, Optimization of an Imidazo[1,2-a] pyridine series to afford highly selective type II/2 dual Mer/Axl kinase inhibitors with in vivo efficacy, J. Med. Chem. 64 (2021) 13524–13539, https://doi.org/10.1021/acs.jmedchem.1c00920.
[26] C. Lecoutey, D. Hedou, T. Freret, P. Giannoni, F. Gaven, M. Since, V. Bouet, C. Ballandonne, S. Corvaisier, A. Malzert Fréon, S. Mignani, T. Cresteil, M. Boulouard, S. Claeysen, C. Rochais, P. Dallemagne, Design of donecopride, a dual serotonin subtype 4 receptor agonist/acetylcholinesterase inhibitor with potential interest for Alzheimer's disease treatment, Proc. Natl. Acad. Sci. USA 111 (2014) E3825–E3830, https://doi.org/10.1073/pnas.1410315111.